Submitted Manuscript: Confidential

Template revised November 2022

Title: Mapping carbon processing in rivers with big data and a global experiment

Authors: S. D. Tiegs[1*#], K. A. Capps[2,3*#], D. M. Costello[4*#], J. P. Schmidt[2*], C. J. Patrick[5*], J. J. Follstad Shah[6], C. J. LeRoy[7], and the CELLDEX Consortium†

[1] Department of Biological Sciences, Oakland University; Rochester, 48309, U.S.A.

[2] Odum School of Ecology, University of Georgia; Athens, 30602, U.S.A.

[3] Savannah River Ecology Laboratory, University of Georgia; Aiken, 29802, U.S.A.

[4] Department of Biological Sciences, Kent State University; Kent, 44242, U.S.A

[5] Virginia Institute of Marine Science, Coastal Ocean Processes Section, William & Mary; Gloucester Point, 23062, U.S.A.

[6] School of the Environment, Society, and Sustainability; University of Utah, Salt Lake City, 84112, U.S.A.

[7] Environmental Studies Program, The Evergreen State College; Olympia, 98505, U.S.A.†CELLDEX Consortium authors and affiliations are listed in the supplementary materials.

***Corresponding authors. Email: tiegs@oakland.edu, kcapps@uga.edu, dcostel3@kent.edu, jps@uga.edu, cpatrick@vims.edu**

[#]These authors contributed equally to this work.

Abstract:

Rivers and streams contribute to global carbon cycling by decomposing immense quantities of terrestrial plant matter. However, decomposition rates are highly variable, and large-scale patterns and drivers of this process remain poorly understood. Using a cellulose-based assay to reflect the primary constituent of plant detritus, we generated a predictive model (81% variance explained) for cellulose-decomposition rates across 514 globally distributed streams. A large number of variables were important for predicting decomposition, highlighting the complexity of this process at the global scale. Predicted cellulose-decomposition rates, when combined with genus-level litter-quality attributes, explain published leaf-litter-decomposition rates with impressive accuracy (70% variance explained). Our global map provides estimates of rates

across vast understudied areas of Earth, and reveals rapid decomposition across continental-scale areas dominated by human activities.

One-Sentence Summary: By integrating big data and a global experiment, we predict organic-matter decomposition in rivers worldwide.

Main Text:

Earth's terrestrial ecosystems produce over 100 billion tons of plant detritus annually (*1*, *2*), and the fates of this organic matter – for example, long-term storage, mineralization to greenhouse gasses, or incorporation into stream food webs – depend on the rate at which it is decomposed. River ecosystems are carbon-processing hotspots (*3*, *4*), receiving 0.72 billion tons of terrestrial carbon per year (*2*), an amount that is disproportionately important relative to the small fraction of non-glaciated land area (0.58%) rivers occupy (*5*). Rivers connect terrestrial ecosystems with aquatic storage compartments including floodplains, lakes and oceans, playing vital roles in the global carbon cycle, and functioning both as organic-matter conduits and reactors. Despite the widely recognized importance of flowing waters in global carbon cycling (*6–8*), our understanding of variation in organic-matter-decomposition rates and their drivers at large spatial scales is still limited (*2*).

Large-scale spatial variation in organic-matter decomposition in rivers and streams has been estimated by comparing leaf-litter-decomposition rates from studies conducted in regions with contrasting climates (*9*, *10*), conducting literature reviews of local field studies (*11*), developing conceptual models (*12*, *13*) and performing meta-analyses (*14*, *15*). Coordinated, distributed experiments (*16–20*) have been particularly insightful by generating directly comparable data across broad geographic areas and identifying coarse-resolution explanatory variables of

decomposition rates in rivers, including differences in decomposer communities and biomes. Still, we lack a comprehensive understanding of how drivers such as climate, geology, vegetation, water quality, and soils interact to govern organic-matter decomposition at large scales. Such knowledge gaps are particularly evident across the tropics and in lower-income economies – ecologically important areas where rivers are grossly understudied relative to those in northern temperate zones. Quantifying patterns and controls of decomposition in these areas is critical, however, because much of Earth's terrestrial plant matter is annually produced in tropical forests (net primary production 16.0–23.1 billion tons of carbon) (*21*, *22*), and tropical rivers deliver 48-64% of the carbon moving from rivers to the ocean (*23*).

Effectively modeling carbon dynamics at the global scale – including areas where field data are scarce – requires a more mechanistic and process-based understanding of the many environmental and biotic factors that drive organic-matter decomposition. Accurate estimates generated by combining existing empirical measurements with fine-scale geospatial and environmental data can provide multiple benefits. They can reduce the need for data collection from remote or difficult-to-access regions, subsequently generating baseline estimates for decomposition in understudied areas of the world. Global-scale predictions also contribute to a finer-scale understanding of decomposition and support efforts to model planetary carbon dynamics. Models that can accurately predict current *in-situ* decomposition rates across space are particularly valuable, enabling manipulation of environmental drivers *in silico* to predict impacts under scenarios of future global environmental change.

Here, we present a predictive model fitted with global data from CELLDEX (Cellulose Decomposition Experiment), a coordinated, distributed experiment on cellulose decomposition

in rivers designed to reveal previously undocumented patterns in decomposition rates and the key factors driving this fundamental ecosystem-level process. Decomposition of cellulose – the most abundant organic polymer on the planet and a main constituent of plant litter – was quantified by over 150 investigators by using a common and well-established cellulose-decomposition assay (*24*). The 'cotton-strip assay' is a standardized approach for measuring decomposition by using a readily available woven cotton fabric (Artist's canvas) that is comprised of 95% cellulose. The loss of tensile strength of the fabric is measured, a process that is strongly correlated with the microbial catabolism of cellulose (*25*). We performed the assay in 514 flowing-water ecosystems at georeferenced field sites on all seven continents, spanning 135º of latitude and each of Earth's major terrestrial biomes (*19*, *20*). We used high-resolution (15 arcsecond) climate, soil, geology, vegetation, and physicochemical data (101 explanatory variables total) in a boosted-regression tree (BRT) algorithm to develop the first global, high-resolution predictive model of organic-matter decomposition in rivers. We then tested the utility of the cellulose model by using predicted cellulose-decomposition rates and genus-level leaf-litter chemistry traits to explain 895 leaf-litter decomposition estimates from studies conducted at 559 unique locations across the globe. We found that cellulose-decomposition rates are an excellent proxy for litter-decomposition rates. Further, our models indicate the physicochemical factors at river and watershed scales interact with characteristics of the organic matter being

decomposed (e.g., leaf-litter chemistry) to create heterogenous spatial patterns in riverine decomposition across the planet.

Climate, geology, soils, and water quality explain cellulose decomposition rates.

Climate, geology, soil, and water-quality variables explain 81% of variance in field measurements of *in-situ* cellulose decomposition. Because a standardized cellulose substrate was used at all field sites, observed variation in decomposition rates can be attributed unequivocally to the activity of microbial communities and environmental drivers. Prior efforts have explained broad variation in decomposition rates across riverine ecosystems as a function of exogenous factors such as temperature (*14*, *19*) and concentrations of dissolved nutrients (*17*, *20*, *26*), as well as litter traits (*15*, *27*, *28*). Our model supports those findings and shows that climatic and water-quality parameters are among the most important explanatory variables of decomposition rates (Fig. 1). However, a relatively large number of explanatory variables (n=26) have importance values greater than 1.0 (table s1), and no single variable contributes >15% to the explanatory power of the model (table s1). This result reveals the complexity of the many drivers that influence organic-matter decomposition at the global scale.

Top explanatory variables of cellulose decomposition include expected attributes like mean daily water temperature (importance value [IV]=14.0; Fig. 1A), nitrogen and phosphorus availability (IV=6.7 and 4.9, respectively; Fig. 1C & D), and mean annual air temperature (IV=2.5; Fig. 1F). Our data and approach also highlight watershed-level characteristics that have been given little attention previously, such as sub-watershed lake area (limnicity) (IV=6.9; Fig. 1B), actual evapotranspiration in the watershed (IV=4.4; Fig. 1E), and the chemical and physical properties of soil (table s1). Subwatershed lake area was a high-ranking variable, and its negative

relationship with decomposition rates may be explained by the disproportionately greater abundance of lakes at high northern latitudes where water temperatures are low (Fig. 1B). Alternatively, lower nutrient concentrations and suppressed hydrological variability may have also contributed to the negative influence of limnicity on decomposition. Although our study sites were selected to have minimal human impacts relative to their region of study (*19*), variables associated with anthropogenic development, such as dissolved-nutrient yields, crop-land extent (IV=2.0), population count (IV=1.3), and river regulation (IV=1.3), still emerge as important (table s1). Notably, relationships between explanatory variables and decomposition rates are frequently non-linear, revealing thresholds beyond which there are abrupt changes in decomposition rates (e.g., Fig. 1B, D, & E). Water temperature has a strong positive effect on cellulose decomposition (Fig. 1A), and there is an optimal range (5-13 °C) of annual air temperature with estimated lower rates in both cooler and warmer watersheds (Fig. 1F).

Extrapolating to global patterns of decomposition rates

Our model and map of riverine cellulose decomposition reveals pronounced, large-scale spatial patterns of organic-matter processing (Fig. 2). Rates generally increase with decreasing latitude, with rapid rates in tropical regions (e.g., Central America, Amazon basin, Western Africa, Indo-Pacific) and areas characterized by volcanic activity and young soils, an effect previously documented only at more local scales (*29*). Importantly, fluvial ecosystems in these regions are among the least studied on the planet (Fig. 2, inset), yet they have high rates of terrestrial primary production (*22*) and carbon export to the ocean (*23*). Vast areas in middle latitudes with ubiquitous human impacts – central Europe, eastern China, central North America, southeastern South America, and Japan – also support elevated decomposition rates, strongly suggesting

continental-scale human impacts on carbon cycling in rivers. In contrast, areas of boreal forests, characterized by short growing seasons, low temperatures, and peaty, acidic, water-logged soils, exhibit slower rates of organic-matter decomposition, especially in northern Asia, eastern Scandinavia, and northeastern Canada.

Validating predicted cellulose-decomposition rates with leaf-litter-decomposition rates

Recognizing that the substrate used in our standardized decomposition assay (cellulose as cotton fabric) lacks the chemical complexity of organic matter that naturally enters running waters, we also tested how accurately our modeling approach could explain variation in the decomposition rates of terrestrial leaf litter in rivers reported by ecologists worldwide. To this end we independently validated model forecasts using 895 unique litter-decomposition rates from 559 locations and representing 35 genera of terrestrial plants (*27*). We also used leaf- and litter-trait data at the genus level (*30*, *31*) and experimental conditions (*14*, *27*) as explanatory variables to account for variation among decomposition estimates resulting from differences in leaf-litter quality (e.g., lignin, hemicellulose, tannin, nutrient content) and the feeding activity of invertebrates (Figure 3A, table s2). Our cellulose-decomposition model predictions coupled with litter traits account for 70% of the variation in leaf-litter decomposition. Importantly, the explanatory power of this model is overwhelmingly driven by predicted rates of cellulose decomposition (IV=39.5), despite the stark differences in quality between the cellulose substrate and natural litter (Fig 3A, table S2). These results provide strong support for the critical

influence that environmental drivers have in regulating riverine litter decomposition, including the drivers impacted by anthropogenic activities.

Prior research at large scales has stressed the importance of litter quality as the predominant control of decomposition rates in rivers (*15*). Our results demonstrate that in addition to leaf-litter traits, environmental factors, such as temperature and nutrient availability, are critically important in regulating decomposition rates at larger spatial scales. Our validation model also reveals that invertebrate access to leaves, as assessed by experimentally manipulating litter-bag mesh size, greatly increase the rate of decomposition in all but the fastest decomposing leaves (Fig. 3A). Finally, litter chemistry contributes to the explanatory power of the model in expected ways, with plant genera that are characterized by high lignin content (IV=11.9; Fig. 3B) and low litter-nitrogen content (C:N, IV=5.45 and N, IV=5.23; Fig. 3C & D) decomposing more slowly. Other litter traits (e.g., P content, cellulose) provide little additional explanatory power and no leaf traits explain more variation than expected by chance (table s2). It is well recognized that leaf-litter chemistry can vary among individuals within a species (*32*, *33*) and even individual leaves from a single tree (*34*); thus, our model may underestimate the importance of individual-level variation in leaf and litter chemistry in driving decomposition. Greater measurement and reporting of litter chemistry, especially nitrogen and lignin content will improve understanding of endogenous controls at global scales. Despite limitations in available data, we show that

cellulose decomposition can be an excellent proxy for litter decomposition, and our composite model of environmental drivers makes reliable estimates of litter decomposition at a global scale.

Forecasting decomposition under global environmental change

The high explanatory power of our cellulose and leaf-litter decomposition models enables forecasting of decomposition rates under altered climate, land cover, soil conditions, and nutrient-loading scenarios. These predictions can identify locations across the globe where decomposition may be particularly susceptible or resistant to global change, thereby informing freshwater-conservation efforts. As proof of concept, we examined potential changes in predicted litter-decomposition rates associated with changes in pine-oak forest composition in Mexican watersheds invaded by pine bark beetle (*Dendroctonus mexicanus*) (*35*). This invasion is expected to be particularly severe in the watershed of the Rio Grande de Santiago, a major conduit of organic matter to the Pacific Ocean in Mexico (Fig. 4). Our forecasts predict that insect-induced canopy replacement from pine to oak would cause decomposition rates to increase and become more variable (2.5- to 3.8-fold increase) with larger increases in decomposition associated with watersheds with greater evapotranspiration and drier soils (fig. s1). To promote the use of our models for forecasting, we created an easy-to-use, open-source online application where users can estimate both cotton-strip and leaf-litter decomposition rates for any river across the globe (https://shiny-bsci.kent.edu/CELLDEX).

Conclusions and implications

By pairing a distributed field experiment with publicly available environmental data, we created the first high-resolution map and predictions of organic-matter decomposition rates in flowing

waters worldwide. Our model demonstrates that cellulose-decomposition results from diverse, interacting, and non-linear environmental forcings that can best be described with complex, data-rich models. Although the standard cotton fabric used lacks the biochemical complexity of leaf litter, our relatively simple organic-matter substrate is an excellent proxy for leaf litter in decomposition studies, as demonstrated by our model predictions. Simplification of the leaf-litter-bag assay allowed us to both achieve standardized results and fill extensive geographic gaps in remote and low-resourced areas, demonstrating the power of coordinated, distributed experiments (*36*). Although our datasets were large when compared against other studies of organic-matter decomposition, the field data used were relatively limited in both space and time, which makes our strong explanatory power all the more striking. Thus, this work also underscores the power of machine-learning algorithms and large geographic databases of environmental data (e.g., HydroBASINS (*37*, *38*)) plus the critical value of temporally and geographically extensive data from simple but standardized coordinated experiments (e.g., CELLDEX).

Given the pressing information needs of measuring ecosystem functions for biomonitoring and bioassessment (*39*, *40*), our globally distributed experiment provides a template for matching observational data with model predictions. This approach provided baseline data for estimated decomposition rates across immense, unstudied areas of the planet, and supports the development of biomonitoring networks in areas where they are most needed (*41*). To further advance large-scale monitoring and assessment we have made these modelling approaches accessible through an open-source online mapping tool. Application of the models to current and

future environmental threats will enable scientists and natural-resource managers to forecast changes in the functioning of river networks at a planetary scale.

Cellulose decomposition is strongly influenced by multiple interacting environmental drivers that continue to be impacted by anthropogenic activities. Undoubtedly, climate change, increased nutrient loading, intensified land-use modification, and changes in vegetation cover will continue to alter organic-matter processing in rivers and streams. Notably, key human-influenced drivers of cellulose decomposition – especially nutrient loading and temperature – are positively related to decomposition rates. A critical implication is that, in the presence of continued environmental change, organic-matter decomposition rates will likely increase in rivers, resulting in declines in shorter-term carbon storage (*42*) and reductions in carbon transfer to longer-term storage compartments, such as reservoirs, floodplains, and oceans.

References

1. J. Cebrian, Patterns in the fate of production in plant communities. *American Naturalist* **154**, 449–468 (1999).
2. T. J. Battin, R. Lauerwald, E. S. Bernhardt, E. Bertuzzo, L. G. Gener, R. O. Hall, E. R. Hotchkiss, T. Maavara, T. M. Pavelsky, L. Ran, P. Raymond, J. A. Rosentreter, P. Regnier, River ecosystem metabolism and carbon biogeochemistry in a changing world. *Nature* **613**, 449–459 (2023).
3. M. E. McClain, E. W. Boyer, C. L. Dent, S. E. Gergel, N. B. Grimm, P. M. Groffman, S. C. Hart, J. W. Harvey, C. A. Johnston, E. Mayorga, W. H. McDowell, G. Pinay, Biogeochemical hot spots and hot moments at the interface of terrestrial and aquatic ecosystems. *Ecosystems* **6,** 301–312 (2003). https://doi.org/10.1007/s10021-003-0161-9.
4. E. R. Hotchkiss, R. O. Hall, R. A. Sponseller, D. Butman, J. Klaminder, H. Laudon, M. Rosvall, J. Karlsson, Sources of and processes controlling CO_2 emissions change with the size of streams and rivers. *Nature Geosciences* **8**, 696–699 (2015).
5. G. H. Allen, T. M. Pavelsky, Global extent of rivers and streams. *Science* **361**, 585–588(2018).
6. P. Regnier, P. Friedlingstein, P. Ciais, F. T. Mackenzie, N. Gruber, I. A. Janssens, G. G. Laruelle, R. Lauerwald, S. Luyssaert, A. J. Andersson, S. Arndt, C. Arnosti, A. V. Borges, A. W. Dale, A. Gallego-Sala, Y. Goddéris, N. Goossens, J. Hartmann, C. Heinze, T. Ilyina, F. Joos, D. E. Larowe, J. Leifeld, F. J. R. Meysman, G. Munhoven, P. A. Raymond, R. Spahni, P. Suntharalingam, M. Thullner, Anthropogenic perturbation of the carbon fluxes from land to ocean. *Nature Geosciences* **6**, 597–607 (2013).
7. A. Marx, J. Dusek, J. Jankovec, M. Sanda, T. Vogel, R. van Geldern, J. Hartmann, J. A. C. Barth, A review of CO_2 and associated carbon dynamics in headwater streams: A global perspective. *Reviews of Geophysics* **55**, 560–585 (2017).
8. P. A. Raymond, J. Hartmann, R. Lauerwald, S. Sobek, C. McDonald, M. Hoover, D. Butman, R. Striegl, E. Mayorga, C. Humborg, P. Kortelainen, H. Dürr, M. Meybeck, P. Ciais, P. Guth, Global carbon dioxide emissions from inland waters. *Nature* **503**, 355–359 (2013).
9. V. Ferreira, A. C. Encalada, M. A. S. Graça, Effects of litter diversity on decomposition and biological colonization of submerged litter in temperate and tropical streams. *Freshwater Science* **31**, 945–962 (2012).
10. A. Bruder, M. H. Schindler, M. S. Moretti, M. O. Gessner, Litter decomposition in a temperate and a tropical stream: The effects of species mixing, litter quality and shredders. *Freshwater Biology* **59**, 438–449 (2014).
11. J. C. Marks, Revisiting the fates of dead leaves that fall into streams. *Annual Review of Ecology, Evolution, and Systematics* **50**, 547–568 (2019).
12. M. A. S. Graça, The role of invertebrates on leaf litter decomposition in streams - A review. *International Review of Hydrobiology: A Journal Covering all Aspects of Limnology and Marine Biology* **86**, 383–393 (2001).
13. T. V. Royer, G. W. Minshall, Controls on leaf processing in streams from spatial-scaling and hierarchical perspectives. *Journal of the North American Benthological Society* **22**, 352–358 (2003).
14. J. J. Follstad Shah, J. S. Kominoski, M. Ardón, W. K. Dodds, M. O. Gessner, N. A. Griffiths, C. P. Hawkins, S. L. Johnson, A. Lecerf, C. J. LeRoy, D. W. P. Manning, A. D. Rosemond, R. L. Sinsabaugh, C. M. Swan, J. R. Webster, L. H. Zeglin, Global synthesis of the temperature sensitivity of leaf litter breakdown in streams and rivers. *Global Change Biology* **23**, 3064–3075 (2017).
15. M. Zhang, X. Cheng, Q. Geng, Z. Shi, Y. Luo, X. Xu, Leaf litter traits predominantly control litter decomposition in streams worldwide. *Global Ecology and Biogeography* **28**, 1469–1486 (2019).
16. L. Boyero, R. G. Pearson, M. O. Gessner, L. A. Barmuta, V. Ferreira, M. A. S. Graça, D. Dudgeon, A. J. Boulton, M. Callisto, E. Chauvet, J. E. Helson, A. Bruder, R. J. Albariño, C. M. Yule, M. Arunachalam, J. N. Davies, R. Figueroa, A. S. Flecker, A. Ramírez, R. G. Death, T. Iwata, J. M. Mathooko, C. Mathuriau, J. F. Gonçalves, M. S. Moretti, T. Jinggut, S. Lamothe, C. M'Erimba, L. Ratnarajah, M. H. Schindler, J. Castela, L. M. Buria, A. Cornejo, V. D. Villanueva, D. C. West, A global experiment suggests climate warming will not accelerate litter decomposition in streams but might reduce carbon sequestration. *Ecology Letters* **14**, 289–294 (2011).
17. G. Woodward, M. O. Gessner, P. S. Giller, V. Gulis, S. Hladyz, A. Lecerf, B. Malmqvist, B. G. McKie, S. D. Tiegs, H. Cariss, M. Dobson, A. Elosegi, V. Ferreira, M. A. S. Graça, T. Fleituch, J. O. Lacoursière, M. Nistorescu, J. Pozo, G. Risnoveanu, M. Schindler, A. Vadineanu, L. B.-M. Vought, E. Chauvet, Continental-scale effects of nutrient pollution on stream ecosystem functioning. *Science* **336**, 1438–1440 (2012).

18. I. T. Handa, R. Aerts, F. Berendse, M. P. Berg, A. Bruder, O. Butenschoen, E. Chauvet, M. O. Gessner, J. Jabiol, M. Makkonen, B. G. McKie, B. Malmqvist, E. T. H. M. Peeters, S. Scheu, B. Schmid, J. Van Ruijven, V. C. A. Vos, S. Hättenschwiler, Consequences of biodiversity loss for litter decomposition across biomes. *Nature* **509**, 218–221 (2014).
19. S. D. Tiegs, D. M. Costello, M. W. Isken, G. Woodward, P. B. McIntyre, M. O. Gessner, E. Chauvet, N. A. Griffiths, A. S. Flecker, V. Acuña, R. Albariño, D. C. Allen, C. Alonso, P. Andino, C. Arango, J. Aroviita, M. V. M. Barbosa, L. A. Barmuta, C. V. Baxter, T. D. C. Bell, B. Bellinger, L. Boyero, L. E. Brown, A. Bruder, D. A. Bruesewitz, F. J. Burdon, M. Callisto, C. Canhoto, K. A. Capps, M. M. Castillo, J. Clapcott, F. Colas, C. Colón-Gaud, J. Cornut, V. Crespo-Pérez, W. F. Cross, J. M. Culp, M. Danger, O. Dangles, E. De Eyto, A. M. Derry, V. D. Villanueva, M. M. Douglas, A. Elosegi, A. C. Encalada, S. Entrekin, R. Espinosa, D. Ethaiya, V. Ferreira, C. Ferriol, K. M. Flanagan, T. Fleituch, J. J. F. Shah, A. F. Barbosa, N. Friberg, P. C. Frost, E. A. Garcia, L. G. Lago, P. E. G. Soto, S. Ghate, D. P. Giling, A. Gilmer, J. F. Gonçalves, R. K. Gonzales, M. A. S. Graça, M. Grace, H.-P. Grossart, F. Guérold, V. Gulis, L. U. Hepp, S. Higgins, T. Hishi, J. Huddart, J. Hudson, S. Imberger, C. Iñiguez-Armijos, T. Iwata, D. J. Janetski, E. Jennings, A. E. Kirkwood, A. A. Koning, S. Kosten, K. A. Kuehn, H. Laudon, P. R. Leavitt, A. L. L. Da Silva, S. J. Leroux, C. J. LeRoy, P. J. Lisi, R. MacKenzie, A. M. Marcarelli, F. O. Masese, B. G. McKie, A. O. Medeiros, K. Meissner, M. Miliša, S. Mishra, Y. Miyake, A. Moerke, S. Mombrikotb, R. Mooney, T. Moulton, T. Muotka, J. N. Negishi, V. Neres-Lima, M. L. Nieminen, J. Nimptsch, J. Ondruch, R. Paavola, I. Pardo, C. J. Patrick, E. T. H. M. Peeters, J. Pozo, C. Pringle, A. Prussian, E. Quenta, A. Quesada, B. Reid, J. S. Richardson, A. Rigosi, J. Rincón, G. Rîşnoveanu, C. T. Robinson, L. Rodríguez-Gallego, T. V. Royer, J. A. Rusak, A. C. Santamans, G. B. Selmeczy, G. Simiyu, A. Skuja, J. Smykla, K. R. Sridhar, R. Sponseller, A. Stoler, C. M. Swan, D. Szlag, F. Teixeira-De Mello, J. D. Tonkin, S. Uusheimo, A. M. Veach, S. Vilbaste, L. B. M. Vought, C.-P. Wang, J. R. Webster, P. B. Wilson, S. Woelfl, M. A. Xenopoulos, A. G. Yates, C. Yoshimura, C. M. Yule, Y. X. Zhang, J. A. Zwart, Global patterns and drivers of ecosystem functioning in rivers and riparian zones. *Sci Adv* **5**, eaav0486 (2019).
20. D. M. Costello, S. D. Tiegs, L. Boyero, C. Canhoto, K. A. Capps, M. Danger, P. C. Frost, M. O. Gessner, N. A. Griffiths, H. M. Halvorson, K. A. Kuehn, A. M. Marcarelli, T. V. Royer, D. M. Mathie, R. J. Albariño, C. P. Arango, J. Aroviita, C. V. Baxter, B. J. Bellinger, A. Bruder, F. J. Burdon, M. Callisto, A. Camacho, F. Colas, J. Cornut, V. Crespo-Pérez, W. F. Cross, A. M. Derry, M. M. Douglas, A. Elosegi, E. de Eyto, V. Ferreira, C. Ferriol, T. Fleituch, J. J. Follstad Shah, A. Frainer, E. A. Garcia, L. García, P. E. García, D. P. Giling, R. K. Gonzales-Pomar, M. A. S. Graça, H.-P. Grossart, F. Guérold, L. U. Hepp, S. N. Higgins, T. Hishi, C. Iñiguez-Armijos, T. Iwata, A. E. Kirkwood, A. A. Koning, S. Kosten, H. Laudon, P. R. Leavitt, A. L. Lemes da Silva, S. J. Leroux, C. J. LeRoy, P. J. Lisi, F. O. Masese, P. B. McIntyre, B. G. McKie, A. O. Medeiros, M. Miliša, Y. Miyake, R. J. Mooney, T. Muotka, J. Nimptsch, R. Paavola, I. Pardo, I. Y. Parnikoza, C. J. Patrick, E. T. H. M. Peeters, J. Pozo, B. Reid, J. S. Richardson, J. Rincón, G. Risnoveanu, C. T. Robinson, A. C. Santamans, G. M. Simiyu, A. Skuja, J. Smykla, R. A. Sponseller, F. Teixeira-de Mello, S. Vilbaste, V. D. Villanueva, J. R. Webster, S. Woelfl, M. A. Xenopoulos, A. G. Yates, C. M. Yule, Y. Zhang, J. A. Zwart, Global patterns and controls of nutrient immobilization on decomposing cellulose in riverine ecosystems. *Global Biogeochemical Cycles* **36**, e2021GB007163 (2022).
21. C. M. Gough, Terrestrial primary production: Fuel for life. *Nature Education Knowledge* **3**, 28 (2011).
22. C. B. Field, M. J. Behrenfeld, J. T. Randerson, P. Falkowski, Primary production of the biosphere: Integrating terrestrial and oceanic components. *Science* **281**, 237–240 (1998).
23. T. H. Huang, Y. H. Fu, P. Y. Pan, C. T. A. Chen, Fluvial carbon fluxes in tropical rivers. *Current Opinion in Environmental Sustainability* **4**, 162–169 (2012).
24. S. D. Tiegs, J. E. Clapcott, N. A. Griffiths, A. J. Boulton, A standardized cotton-strip assay for measuring organic-matter decomposition in streams. *Ecological Indicators* **32**, 131–139 (2013).
25. J. Mancuso, J. L. Tank, U. H. Mahl, A. Vincent, S. D. Tiegs, Monthly variation in organic-matter decomposition in agricultural stream and riparian ecosystems. *Aquatic Sciences* **85**, 83 (2023).
26. M. Ardón, L. H. Zeglin, R. M. Utz, S. D. Cooper, W. K. Dodds, R. J. Bixby, A. S. Burdett, J. Follstad Shah, N. A. Griffiths, T. K. Harms, S. L. Johnson, J. B. Jones, J. S. Kominoski, W. H. McDowell, A. D. Rosemond, M. T. Trentman, D. Van Horn, A. Ward, Experimental nitrogen and phosphorus enrichment stimulates multiple trophic levels of algal and detrital-based food webs: A global meta-analysis from streams and rivers. *Biological Reviews* **96**, 692–715 (2021).

27. C. J. LeRoy, A. L. Hipp, K. Lueders, J. J. Follstad Shah, J. S. Kominoski, M. Ardón, W. K. Dodds, M. O. Gessner, N. A. Griffiths, A. Lecerf, D. W. P. Manning, R. L. Sinsabaugh, J. R. Webster, Plant phylogenetic history explains in-stream decomposition at a global scale. *Journal of Ecology* **108**, 17–35 (2020).
28. K. Yue, P. De Frenne, K. Van Meerbeek, V. Ferreira, D. A. Fornara, Q. Wu, X. Ni, Y. Peng, D. Wang, P. Heděnec, Y. Yang, F. Wu, J. Peñuelas, Litter quality and stream physicochemical properties drive global invertebrate effects on instream litter decomposition. *Biological Reviews* **97**, 2023–2038 (2022).
29. A. D. Rosemond, C. M. Pringle, A. Ramírez, M. J. Paul, J. L. Meyer, Landscape variation in phosphorus concentration and effects on detritus-based tropical streams. *Limnology and Oceanography* **47**, 278–289 (2002).
30. L. Boyero, M. A. S. Graça, A. M. Tonin, J. Pérez, A. J. Swafford, V. Ferreira, A. Landeira-Dabarca, M. A. Alexandrou, M. O. Gessner, B. G. McKie, R. J. Albariño, L. A. Barmuta, M. Callisto, J. Chará, E. Chauvet, C. Colón-Gaud, D. Dudgeon, A. C. Encalada, R. Figueroa, A. S. Flecker, T. Fleituch, A. Frainer, J. F. Gonçalves, J. E. Helson, T. Iwata, J. Mathooko, C. M'Erimba, C. M. Pringle, A. Ramírez, C. M. Swan, C. M. Yule, R. G. Pearson, Riparian plant litter quality increases with latitude. *Scientific Reports* **7**, 10562 (2017).
31. J. Kattge, S. Díaz, S. Lavorel, I. C. Prentice, P. Leadley, G. Bönisch, E. Garnier, M. Westoby, P. B. Reich, I. J. Wright, J. H. C. Cornelissen, C. Violle, S. P. Harrison, P. M. Van Bodegom, M. Reichstein, B. J. Enquist, N. A. Soudzilovskaia, D. D. Ackerly, M. Anand, O. Atkin, M. Bahn, T. R. Baker, D. Baldocchi, R. Bekker, C. C. Blanco, B. Blonder, W. J. Bond, R. Bradstock, D. E. Bunker, F. Casanoves, J. Cavender-Bares, J. Q. Chambers, F. S. Chapin, J. Chave, D. Coomes, W. K. Cornwell, J. M. Craine, B. H. Dobrin, L. Duarte, W. Durka, J. Elser, G. Esser, M. Estiarte, W. F. Fagan, J. Fang, F. Fernández-Méndez, A. Fidelis, B. Finegan, O. Flores, H. Ford, D. Frank, G. T. Freschet, N. M. Fyllas, R. V. Gallagher, W. A. Green, A. G. Gutierrez, T. Hickler, S. I. Higgins, J. G. Hodgson, A. Jalili, S. Jansen, C. A. Joly, A. J. Kerkhoff, D. Kirkup, K. Kitajima, M. Kleyer, S. Klotz, J. M. H. Knops, K. Kramer, I. Kühn, H. Kurokawa, D. Laughlin, T. D. Lee, M. Leishman, F. Lens, T. Lenz, S. L. Lewis, J. Lloyd, J. Llusià, F. Louault, S. Ma, M. D. Mahecha, P. Manning, T. Massad, B. E. Medlyn, J. Messier, A. T. Moles, S. C. Müller, K. Nadrowski, S. Naeem, Ü. Niinemets, S. Nöllert, A. Nüske, R. Ogaya, J. Oleksyn, V. G. Onipchenko, Y. Onoda, J. Ordoñez, G. Overbeck, W. A. Ozinga, S. Patiño, S. Paula, J. G. Pausas, J. Peñuelas, O. L. Phillips, V. Pillar, H. Poorter, L. Poorter, P. Poschlod, A. Prinzing, R. Proulx, A. Rammig, S. Reinsch, B. Reu, L. Sack, B. Salgado-Negret, J. Sardans, S. Shiodera, B. Shipley, A. Siefert, E. Sosinski, J. F. Soussana, E. Swaine, N. Swenson, K. Thompson, P. Thornton, M. Waldram, E. Weiher, M. White, S. White, S. J. Wright, B. Yguel, S. Zaehle, A. E. Zanne, C. Wirth, TRY - A global database of plant traits. *Global Change Biology* **17**, 2905–2935 (2011).
32. C. J. LeRoy, T. G. Whitham, S. C. Wooley, J. C. Marks, Within-species variation in foliar chemistry influences leaf-litter decomposition in a Utah river. *Journal of the North American Benthological Society* **26**, 426–438 (2007).
33. A. Lecerf, E. Chauvet, Intraspecific variability in leaf traits strongly affects alder leaf decomposition in a stream. *Basic and Applied Ecology* **9**, 598–605 (2008).
34. T. Sariyildiz, J. M. Anderson, Decomposition of sun and shade leaves from three deciduous tree species, as affected by their chemical composition. *Biology and Fertility of Soils* **37**, 137–146 (2003).
35. A. González-Hernández, R. Morales-Villafaña, M. E. Romero-Sánchez, B. Islas-Trejo, R. Pérez-Miranda. Modelling potential distribution of a pine bark beetle in Mexican temperate forests using forecast data and spatial analysis tools. *J For Res*, **31**, 649–659 (2020).
36. L. H. Fraser, H. Al Henry, C. N. Carlyle, S. R. White, C. Beierkuhnlein, J. F. Cahill, B. B. Casper, E. Cleland, S. L. Collins, J. S. Dukes, A. K. Knapp, E. Lind, R. Long, Y. Luo, P. B. Reich, M. D. Smith, M. Sternberg, R. Turkington, Coordinated distributed experiments: An emerging tool for testing global hypotheses in ecology and environmental science. *Frontiers in Ecology and the Environment* **11**, 147–155 (2013).
37. B. Lehner, K. Verdin, A. Jarvis, New global hydrography derived from spaceborne elevation data. *Eos, Transactions American Geophysical Union* **89**, 93–94 (2008).
38. B. Lehner, G. Grill, Global river hydrography and network routing: Baseline data and new approaches to study the world's large river systems. *Hydrological Processes* **27**, 2171–2186 (2013).
39. M. O. Gessner, E. Chauvet, A case for using litter breakdown to assess functional stream integrity. *Ecological Applications* **12**, 498–510 (2002).

40. M. C. Jackson, O. L. F. Weyl, F. Altermatt, I. Durance, N. Friberg, A. J. Dumbrell, J. J. Piggott, S. D. Tiegs, K. Tockner, C. B. Krug, P. W. Leadley, G. Woodward, Recommendations for the next generation of global freshwater biological monitoring tools. *Advances in Ecological Research* **55**, 615–636 (2016).
41. K. A. Wilson, N. A. Auerbach, K. Sam, A. G. Magini, A. S. L. Moss, S. D. Langhans, S. Budiharta, D. Terzano, E. Meijaard, Conservation research is not happening where it is most needed. *PLoS Biology* **14**, e1002413 (2016).
42. A. D. Rosemond, J. P. Benstead, P. M. Bumpers, V. Gulis, J. S. Kominoski, D. W. P. Manning, K. Suberkropp, J. B. Wallace, Experimental nutrient additions accelerate terrestrial carbon loss from stream ecosystems. *Science* **347**, 1142–1145 (2015).
43. D. Costello, J. P. Schmidt, C. Patrick, K. Capps, J. Follstad Shah, C. LeRoy, and S.D. Tiegs. Data from: Mapping carbon processing in rivers with big data and a global experiment, Zenodo (2024); https://zenodo.org/doi/10.5281/zenodo.10688947
44. J. Cheng, B. Schloerke, B. Karambelkar, Y. Xie, leaflet: Create Interactive Web Maps with the JavaScript "Leaflet" Library, version 2.2.1, Comprehensive R Archive Network (2023); https://cran.r-project.org/package=leaflet
45. A. N. Strahler, Quantitative analysis of watershed geomorphology. *Eos, Transactions American Geophysical Union* **38**, 913–920 (1957).
46. R. W. McDowell, A. Noble, P. Pletnyakov, L. M. Mosley, Global database of diffuse riverine nitrogen and phosphorus loads and yields. *Geoscience Data Journal* **8**, 132–143 (2021).
47. D. Ackerman, D. B. Millet, X. Chen, Global estimates of inorganic nitrogen deposition across four decades. *Global Biogeochemical Cycles* **33**, 100–107 (2019).
48. J. Brahney, N. Mahowald, D. S. Ward, A. P. Ballantyne, J. C. Neff, Is atmospheric phosphorus pollution altering global alpine Lake stoichiometry? *Global Biogeochemical Cycles* **29**, 1369–1383 (2015).
49. N. Mahowald, T. D. Jickells, A. R. Baker, P. Artaxo, C. R. Benitez-Nelson, G. Bergametti, T. C. Bond, Y. Chen, D. D. Cohen, B. Herut, N. Kubilay, R. Losno, C. Luo, W. Maenhaut, K. A. McGee, G. S. Okin, R. L. Siefert, S. Tsukuda, Global distribution of atmospheric phosphorus sources, concentrations and deposition rates, and anthropogenic impacts. *Global Biogeochemical Cycles* **22**, GB4026 (2008).
50. J. Elith, J. R. Leathwick, T. Hastie, A working guide to boosted regression trees. *Journal of Animal Ecology* **77**, 802–813 (2008).
51. R Core Team. R: A language and environment for statistical computing, version 4.3.2. Comprehensive R Archive Network (2023); https://www.R-project.org/
52. G. Ridgeway, GBM Developers. gbm: Generalized boosted regression models, version 2.1.9, Comprehensive R Archive Network (2024); https://cran.r-project.org/package=gbm
53. L. Breiman, Random forests. *Machine Learning* **45**, 5–32 (2001).
54. A. M. Thorn, J. R. Thompson, J. S. Plisinski, Patterns and predictors of recent forest conversion in New England. *Land* **5**, 30 (2016).
55. R. J. Hijmans, raster: Geographic data analysis and modeling, version 3.6-36, Comprehensive R Archive Network (2023); https://cran.r-project.org/package=raster

Acknowledgments: We are grateful for the efforts of the many people who assisted with the CELLDEX project in the lab and in the field, for Jasmine Mancuso for edits on an earlier version of this manuscript, Diane Ethaiya for logistical assistance during the CELLDEX project, and Joshua Talbott for assistance with the Shiny application. Any use of trade, firm, or product names is for descriptive purposes only and does not imply endorsement by the U.S. Government.

Funding: This work was sponsored by an Ecuadorian National Science Foundation PROMETEO award to ST. Original data compilation of leaf litter decomposition rates from primary literature was supported by a working group grant to JFS from the U.S. National Science Foundation (Division of Environmental Biology #1545288 and #1929393) through the U.S. Long Term Ecological Research Network. A portion of the salary of KAC was supported by the

Department of Energy Office of Environmental Management under Award Number DE-EM0005228 to the University of Georgia Research Foundation.

Author contributions:

Conceptualization: DC, JPS, KC, ST

Methodology: CP, DC, JPS, KC, ST

Investigation: All co-authors. CL and JFS also provided data from a literature review

Visualization: DC, JPS

Funding acquisition: ST

Writing – original draft: KC, ST

Writing – review and editing: BM, CP, DC, FB, JPS, KC, MG, NG, ST, GW

Competing interests/Disclaimer: Authors declare that they have no competing interests.

Data and materials availability: All data and code for analyses and figures are available on GitHub (*43*).

Fig. 1. Partial-dependence plots (black lines) of the top variables that explain and predict cellulose-decomposition rates (K_d). Background maps show global distributions of explanatory variables in Mollweide projection. The boosted-regression tree model explains 81% of the variance in decomposition rates across the 514 streams used in our study. Most top variables relate to climate and water quality and effects exhibit non-linear threshold responses. Black ticks above the x-axis indicate decile breaks.

Fig. 2. Predicted mean annual cellulose-decomposition rates (K_d) revealing broad spatial patterns in decomposition rates. We did not predict K_d for sub-watersheds with ≤10 ha of sub-basin area, nor for Antarctica, for which we did not have values for most predictor variables. Inset shows study sites for cellulose (light-filled circles) and leaf-litter (dark-filled circles) decomposition measurements. Map and insert are Mollweide projection.

Fig. 3. Partial-dependence plots of the top variables that explain leaf-litter-decomposition rates (K_d). The boosted-regression-tree model explains 70% of the variance in rates across 895 published values of leaf-litter decomposition and leaf quality (*27*). Top explanatory variables included our modeled cellulose-decomposition rates, invertebrate access to the leaf material, and attributes related to litter quality. Smooth fits (GAM) show the relationship between cellulose-decomposition rate and litter decomposition for the two different common litter-bag mesh sizes that allow or exclude invertebrates (A). The smooth fits capture the general environmental effects on decomposition, whereas the partial dependency plots (thin lines) are noisier due to covariation in leaf quality and environmental conditions (i.e., certain leaf types are used in

certain regions). Black ticks above *x*-axis indicate decile breaks. Note the change in *y*-axis between panel A and B-C.

Fig. 4. Distribution of temperate-coniferous forests in Mexico (all points) and locations (orange) where there is a moderate-to-high risk of pine bark beetle (*Dendroctonus mexicanus*) invasion (adapted from (*35*)) that drives a shift from coniferous to deciduous forest. Inset shows the density distribution of predicted litter-decomposition rates for streams in areas of moderate-to-high invasion risk both for pine litter (green solid line) and oak litter (orange dashed line). Our model predicts that full canopy replacement from pine to oak would increase leaf-litter decomposition rates 2.5- to 3.8-fold with a greater increase predicted in watersheds with greater evapotranspiration and drier soils. Base from U.S. Geological Survey, The National Map, 2023; Web Mercator projection; created in the R package leaflet 2.2.1 (*44*).

List of Supplemental Materials (SM):

CELLDEX Consortium Authors and Affiliations
Materials and Methods
Figure S1
Tables S1 and S2
References (*45-55*)

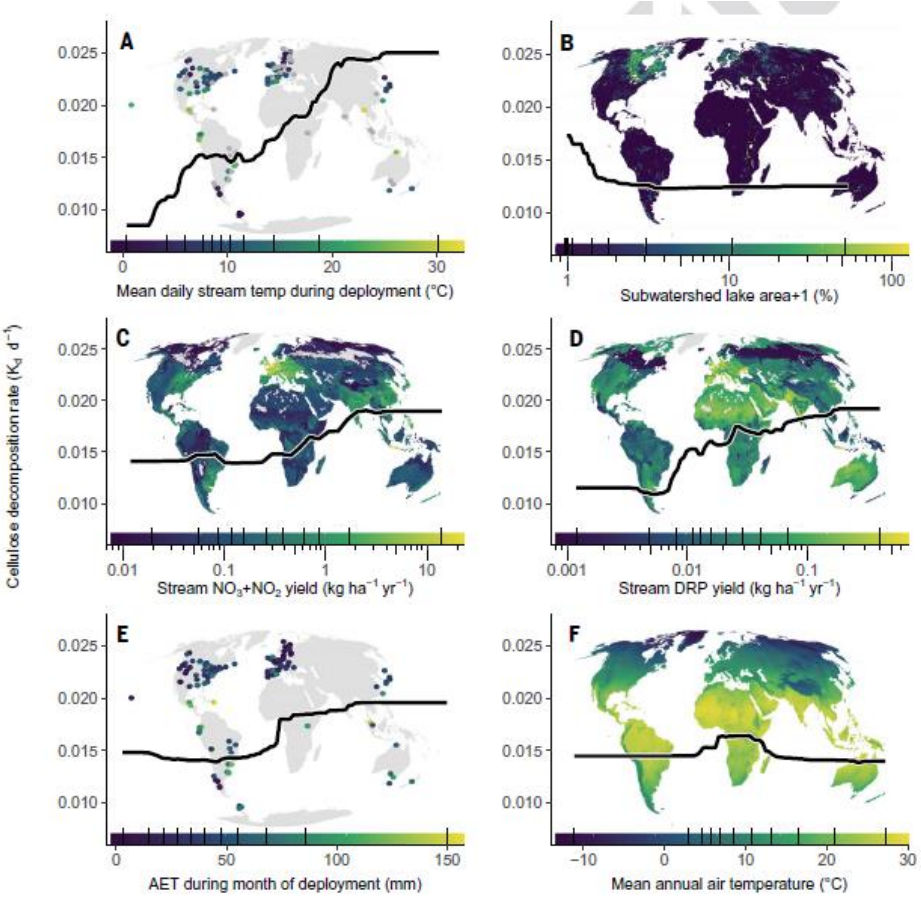

Fig. 1. Partial dependence plots (black lines) of the top variables that explain and predict cellulose decomposition rates (K_d). Background maps show global distributions of explanatory variables in a Mollweide projection. The boosted regression tree model explains 81% of the variance in decomposition rates across the 514 streams used in our study. Most top variables relate to climate and water quality and effects exhibit nonlinear threshold responses. Black ticks above the *x*-axis indicate decile breaks.

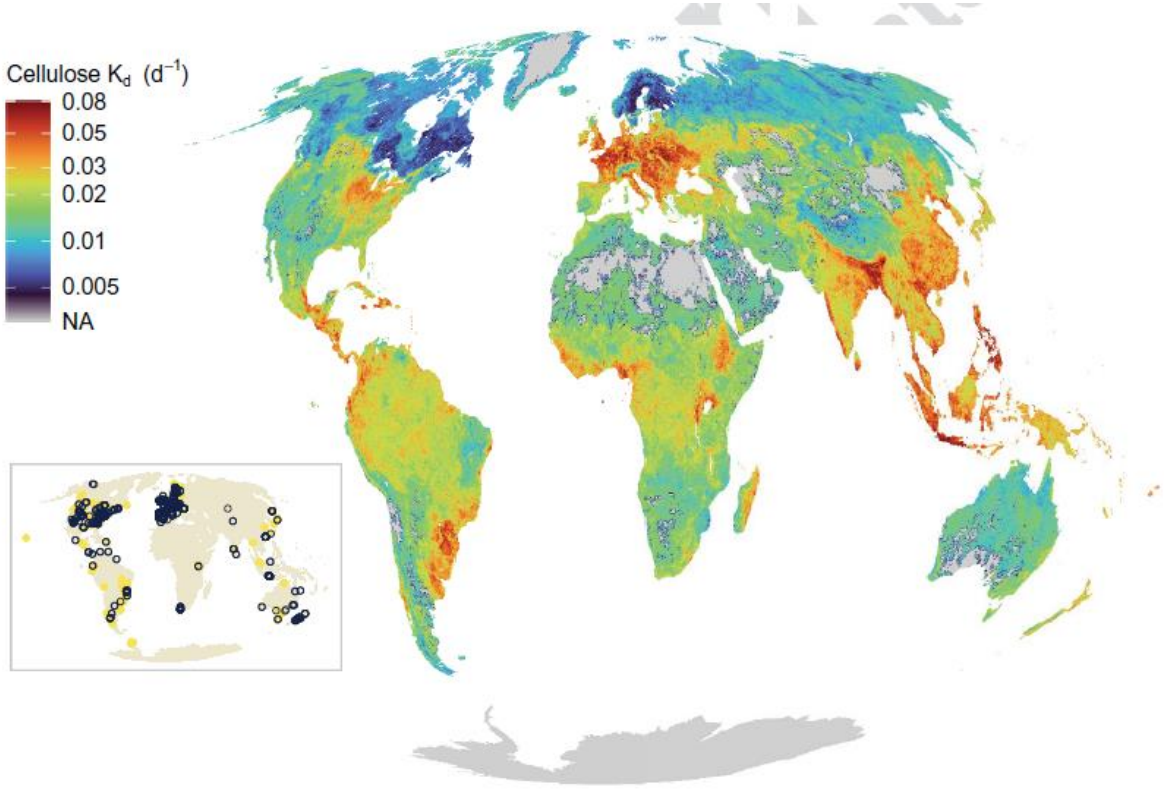

Fig. 2. Predicted mean annual cellulose decomposition rates (K_d) revealing broad spatial patterns in decomposition rates. We did not predict K_d for sub watersheds with ≤10 ha of sub basin area, nor for Antarctica, for which we did not have values for most predictor variables. Inset shows study sites for cellulose (light filled circles) and leaf litter (dark filled circles) decomposition measurements. Map and insert are Mollweide projection.

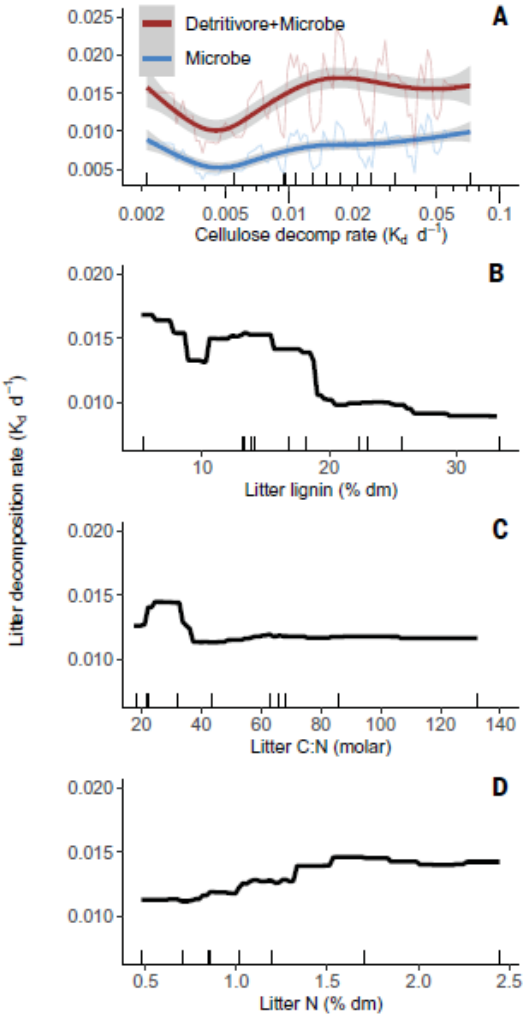

Fig. 3. Partial dependence plots of the top variables that explain leaf litter decomposition rates (K_d). The boosted regression tree model explains 70% of the variance in rates across 895 published values of leaf litter decomposition and leaf quality (*27*). Top explanatory variables included our modeled cellulose decomposition rates, invertebrate access to the leaf material, and attributes related to litter quality. Smooth fits (GAM) show the relationship between cellulose decomposition rate and litter decomposition for the two different common litter bag mesh sizes that allow or exclude invertebrates (A). The smooth fits capture the general environmental effects on decomposition, whereas the partial dependency plots (thin lines) are noisier due to covariation in leaf quality and environmental conditions (i.e., certain leaf types are used in certain regions). Black ticks above *x* axis indicate decile breaks. Note the change in *y* axis between panel A and B C.

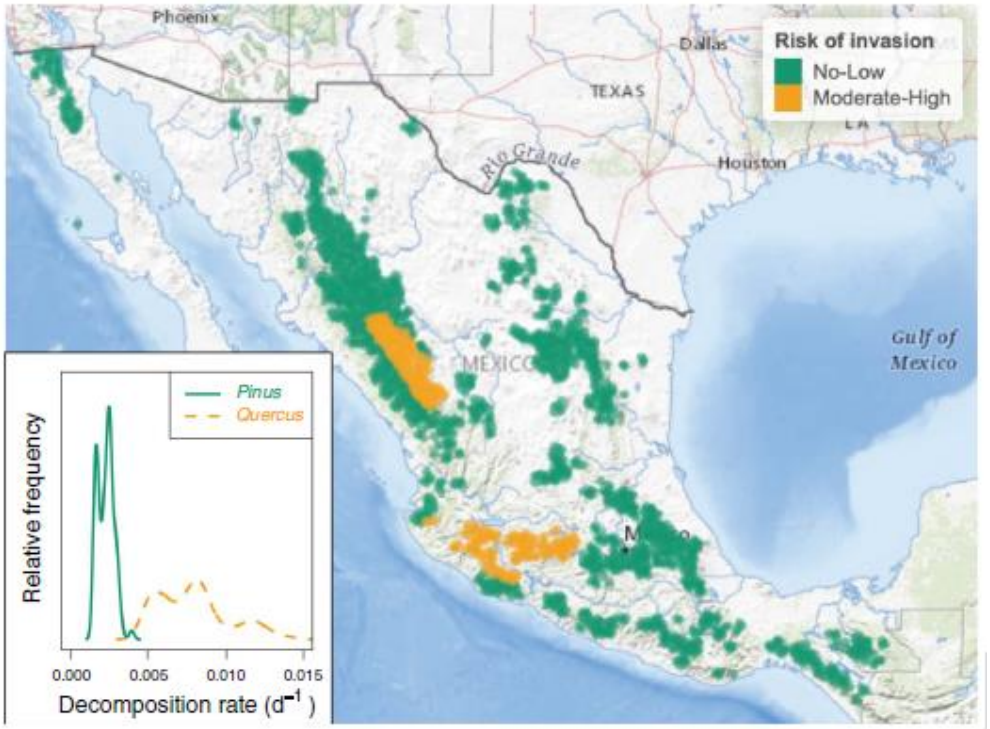

Fig. 4. Distribution of temperate coniferous forests in Mexico (all points) and locations (orange) where there is a moderate to high risk of pine bark beetle (Dendroctonus mexicanus) invasion (adapted from (35)) that drives a shift from coniferous to deciduous forest. Inset shows the density distribution of predicted litter decomposition rates for streams in areas of moderate to high invasion risk both for pine litter (green solid line) and oak litter (orange dashed line). Our model predicts that full canopy replacement from pine to oak would increase leaf litter decomposition rates 2.5 to 3.8 fold with a greater increase predicted in watersheds with greater evapotranspiration and drier soils. Base from U.S. Geological Survey, The National Map, 2023;Web Mercator projection; created in the R package leaflet 2.2.1 (44).

Submitted Manuscript: Confidential

Template revised November 2022

Supplementary Materials for

Mapping carbon processing in rivers with big data and a global experiment

Scott D. Tiegs *et al.*

Corresponding authors: Scott Tiegs, tiegs@oakland.edu; Krista A. Capps, kcapps@uga.edu; David M. Costello, dcostel3@kent.edu; John P. Schmidt, jps@uga.edu; Christopher J. Patrick, cpatrick@vims.edu

The PDF file includes:

CELLDEX Consortium Authors and Affiliations

Scott D. Tiegs[1], Krista A. Capps[2,3], David M. Costello[4], John Paul Schmidt[2], Christopher J. Patrick[5], Jennifer J. Follstad Shah[6], Carri J. LeRoy[7], Vicenç Acuña[8], Ricardo Albariño[9], Daniel C. Allen[10], Cecilia Alonso[11], Patricio Andino[12], Clay Arango[13], Jukka Aroviita[14], Marcus V.M. Barbosa[15], Leon A. Barmuta[16], Colden Baxter[17], Brent Bellinger[18], Luz Boyero[19], Lyubov Bragina[20], Lee E. Brown[21], Andreas Bruder[22], Denise A. Bruesewitz[23], Francis Burdon[24], Marcos Callisto[25], Antonio Camacho[26], Cristina Canhoto[27], María M. Castillo[28], Eric Chauvet[29], Joanne Clapcott[30], Fanny Colas[31], Checo Colón-Gaud[32], Julien Cornut[22], Verónica Crespo-Pérez[12], Wyatt F. Cross[33], Joseph Culp[34], Michael Danger[35], Olivier Dangles[36], Elvira de Eyto[37], Alison M. Derry[38], Veronica Díaz Villanueva[9], Michael M. Douglas[39], Arturo Elosegi[19], Andrea C. Encalada[40], Sally Entrekin[41], Rodrigo Espinosa[42], Verónica Ferreira[27], Carmen Ferriol[43], Kyla M. Flanagan[44], Alexander S. Flecker[45], Tadeusz Fleituch[46], André Frainer[47,48], Nikolai Friberg[49], Paul C. Frost[50], Erica A. Garcia[51], Liliana García-Lago[52], Pavel Ernesto García Soto[53], Mark O. Gessner[54,55], Sudeep Ghate[56], Darren P. Giling[57,58], Alan Gilmer[59], José Francisco Gonçalves Jr[60], Rosario Karina Gonzales[61], Manuel A.S. Graça[27], Mike Grace[62], Natalie A. Griffiths[63], Hans-Peter Grossart[55,64], François Guérold[35], Vlad Gulis[65], Pablo E. Gutiérrez-Fonseca[66], Luiz U. Hepp[67], Scott Higgins[68], Takuo Hishi[69], Joseph Huddart[70], John Hudson[71], Moss Imberger[72], Carlos Iñiguez-Armijos[73], Mark W. Isken[74], Tomoya Iwata[75], David J. Janetski[76], Andrea E. Kirkwood[77], Aaron A. Koning[78], Sarian Kosten[79], Kevin A. Kuehn[80], Hjalmar Laudon[81], Peter R. Leavitt[82], Aurea L Lemes da Silva[83], Shawn Leroux[84], Peter J. Lisi[85], Richard MacKenzie[86], Amy M. Marcarelli[87], Frank O. Masese[88], Peter B. McIntyre[89], Brendan G. McKie[90], Adriana Medeiros[91], Kristian Meissner[92], Marko Miliša[93], Shailendra Mishra[94], Yo Miyake[95], Ashley Moerke[96], Shorok Mombrikotb[70], Rob Mooney[97], Timothy Moulton[98], Timo Muotka[99], Junjiro Negishi[100], Vinicius Neres-Lima[101], Mika L. Nieminen[102], Jorge Nimptsch[103], Jakub Ondruch[104], Riku Paavola[105,106], Isabel Pardo[52], Edwin T.H.M. Peeters[107], Jesus Pozo[19], Aaron Prussian[108], Estefania Quenta[61], Brian Reid[109], John S. Richardson[110], Anna Rigosi[111], José Rincón[112], Geta Risnoveanu[113], Christopher T. Robinson[114,115], Lorena Rodríguez-Gallego[11], Todd V. Royer[116], James A. Rusak[117], Anna C. Santamans[26], Géza B. Selmeczy[118,119], Gelas Simiyu[88], Agnija Skuja[120], Jerzy Smykla[46], Ryan Sponseller[121], Kandikere R. Sridhar[122], Aaron Stoler[123], Christopher M. Swan[124], Franco Teixeira-de Mello[125], Jonathan D. Tonkin[126,127]Sari Uusheimo[128], Allison M. Veach[129], Sirje Vilbaste[130], Lena B.-M. Vought[131], Chiao-Ping Wang[132], Jackson R. Webster[133], Paul B.Wilson[134], Stefan Woelfl[103], Guy Woodward[70], Marguerite A. Xenopoulos[50], Adam G. Yates[135], Chihiro Yoshimura[136], Catherine M. Yule[137], Yixin Zhang[138], Jacob A. Zwart[139]

[1]Biological Sciences, Oakland University; Rochester, 48309, USA.

[2]Odum School of Ecology, University of Georgia; Athens, 30606, USA.

[3]Savannah River Ecology Laboratory, University of Georgia; Aiken, 29802, USA.

[4]Department of Biological Sciences, Kent State University; Kent, 44242, USA.

[5]Coastal Ocean Processes Section, Virginia Institute of Marine Science, William & Mary; Gloucester Point, 23062, USA.

[6]School of Environment, Society, and Sustainability, University of Utah; Salt Lake City, 84112, USA.

[7]Environmental Studies Program, The Evergreen State College; Olympia, 98505, USA.

[8]Catalan Institute for Water Research; Girona, 17003, Spain.

[9]Lab. Limnology, Instituto de Investigaciones en Biodiversidad y Medio Ambiente; Bariloche, 8400, Argentina.

[10]Department of Ecosystem Science and Management, Penn State University; University Park, 16802, USA

[11]Departamento Interdisciplinario de Sistemas Costeros y Marinos, Centro Universitario Regional del Este-Universidad de la República; Rocha, 27000, Uruguay.

[12]School of Biological Sciences, Pontifical Catholic University of Ecuador; Quito, 170525, Ecuador.

[13]Department of Biological Sciences, Central Washington University; Ellensburg, 98926, USA.

[14]Marine and Freshwater Solutions, Finnish Environment Institute; Oulu, 90014, Finland.

[15]Department of Biology, University of Gurupi; Paraíso do Tocantins, 77600, Brazil.

[16]Biological Sciences, School of Natural Sciences, University of Tasmania; Hobart, 7001, Australia.

[17]Stream Ecology Center, Department of Biological Sciences, Idaho State University; Pocatello, 83201, USA.

[18]Watershed Protection Department, City of Austin; Austin, 78704, USA.

[19]Department of Plant Biology and Ecology, University of the Basque Country; Leioa, 48940, Spain.

[20]Animal & Grassland Research Centre, Teagasc; Athenry, Co.; Galway, H65 R718, Ireland.

[21]School of Geography and water@leeds, University of Leeds; Leeds, LS2 9JT, UK.

[22]Institute of Microbiology, University of Applied Sciences and Arts of Southern Switzerland; Mendrisio, 6850, Switzerland.

[23]Environmental Studies Department, Colby College; Waterville, 04901, USA.

[24]School of Science, University of Waikato; Hamilton, 3216, New Zealand.

[25]Departamento de Genética, Ecologia e Evolução, Universidade Federal de Minas Gerais; Belo Horizonte, 30840-430, Brazil.

[26]Cavanilles Institute of Biodiversity and Evolutionary Biology, University of Valencia; Paterna, E46980, Spain.

[27]Marine and Environmental Sciences Centre, Aquatic Research Network, Department of Life Sciences, University of Coimbra; Coimbra, 3000-456, Portugal.

[28]Departamento de Ciencias de la Sustentabilidad, El Colegio de la Frontera Sur; Villahermosa, 86280, Mexico.

[29]Laboratoire Écologie Fonctionnelle et Environnement, Université de Toulouse; Toulouse, 31062, France.

[30]Freshwater Group, Cawthron Institute; Nelson, 7010, New Zealand.

[31]Université Claude Bernard Lyon 1, LEHNA UMR 5023, CNRS, ENTPE; Villeurbanne, F-69622, France.

[32]Department of Biology, Georgia Southern University; Statesboro, 30458, USA.

[33]Department of Ecology, Montana State University; Bozeman, 59715, USA.

[34]Department of Biology, Wilfrid Laurier University; Waterloo, N2L 3E5, Canada.

[35]Laboratoire Interdisciplinaire des Environnements Continentaux CNRS, University of Lorraine; Metz, 57000, France.

[36]CEFE, Univ Montpellier, IRD, CNRS, EPHE; Montpellier, 34000, France.

[37]Fisheries Ecosystems Advisory Services, Marine Institute; Newport, F28PF65, Ireland.

[38]Département des Sciences Biologiques, Université du Québec à Montréal; Montréal, H2X1Y4, Canada.

[39]School of Agriculture and Environment, University of Western Australia; Crawley, 6009, Australia.

[40]College of Biological and Environmental Sciences, Universidad San Francisco de Quito; Quito,170901, Ecuador.

[41]Department of Entomology, Virginia Tech University; Blacksburg, 24060, USA.

[42]Biogeography and Spatial Ecology Research Group, Universidad Regional Amazónica Ikiam; Tena, 150101, Ecuador.

[43]Department of Microbiology and Ecology, University of Valencia, Burjassot, E46100, Spain.

[44]Department of Biological Sciences, University of Calgary; Calgary, T2N 1N4, Canada.

[45]Department of Ecology and Evolutionary Biology, Cornell University; Ithaca, 14853, USA.

[46]Department of Biodiversity, Institute of Nature Conservation Polish Academy of Sciences; Kraków, 31-120, Poland.

[47] Norwegian Institute for Nature Research (NINA), University of Tromsø; Tromsø, 7485, Norway.

[48]Department of Arctic and Marine Biology, UiT the Arctic University of Norway; Tromsø, 9037, Norway.

[49]Department of Ecoscience, Aarhus University; Aarhus, 8000 C, Denmark.

[50]Department of Biology, Trent University; Peterborough, K9L 0G2, Canada.

[51]Research Institute for the Environment and Livelihoods, Charles Darwin University; Casuarina, 0909, Australia.

[52]Department of Ecology and Animal Biology, University of Vigo; Vigo, 36310, Spain.

[53]Escuela de Biología, Universidad de San Carlos de Guatemala; Ciudad de Guatemala, 01012, Guatemala.

[54]Department of Ecology, Berlin Institute of Technology (TU Berlin); Berlin, 10587, Germany.

[55]Department of Plankton and Microbial Ecology, Leibniz Institute of Freshwater Ecology and Inland Fisheries (IGB); Stechlin, 16775, Germany.

[56]Center for Bioinformatics, NITTE Deemed to be University; Mangaluru,575018, India.

[57]Centre for Applied Water Science, Institute for Applied Ecology, Faculty of Science and Technology, University of Canberra; Canberra, 2617, Australia.

[58]Department of Plankton and Microbial Ecology, Leibniz Institute of Freshwater Ecology and Inland Fisheries; Stechlin, 16775, Germany.

[59]Environmental Sustainability & Health Institute, Technological University Dublin; Dublin, DO7 H6K8, Ireland.

[60]Department of Ecology, University of Brasília; Brasilia, 70910-900, Brazil.

[61]Unidad de Ecología Acuática of the Instituto de Ecología, Universidad Mayor de San Andrés; La Paz, La Paz, Bolivia.

[62]School of Chemistry, Monash University; Clayton, 3800, Australia.

[63]Environmental Sciences Division, Oak Ridge National Laboratory; Oak Ridge, 37831, USA.

[64]Institute of Biochemistry and Biology, Potsdam University; Potsdam, 14469, Germany.

[65]Department of Biology, Coastal Carolina University; Conway, 29528, USA.

[66]Rubenstein School of Environment and Natural Resources, University of Vermont; Burlington, 05405, USA.

[67]Federal University of Mato Grosso do Sul; Três Lagoas, 79613-000, Brazil.

[68]Experimental Lakes Area, International Institute for Sustainable Development; Winnipeg, R3B 0T4, Canada.

[69]Kyushu University Forest, Kyushu University; Sasaguri Fukuoka, 8112415, Japan.

[70]Department of Life Sciences, Imperial College London; London, SW7 2AZ, England.

[71]Unaffiliated; Juneau, 99801, USA.

[72]School of Agriculture, Food and Ecosystem Sciences, The University of Melbourne; Burnley, 3121, Australia.

[73]Laboratorio de Ecología Tropical y Servicios Ecosistémicos, Universidad Técnica Particular de Loja; Loja, 1101608, Ecuador.

[74]Decision and Information Sciences, Oakland University; Rochester, 48309, USA.

[75]Faculty of Life and Environmental Sciences, University of Yamanashi; Kofu, 400-8510, Japan.

[76]Department of Biology, Indiana University of Pennsylvania; Indiana, 15705, USA.

[77]Faculty of Science, Ontario Tech University; Oshawa, L1G 0C5, Canada.

[78]Department of Biology, University of Nevada, Reno; Reno, 89557, USA.

[79]Department of Ecology, Radboud Institute for Biological and Environmental Sciences, Radboud University; Nijmegen, 6525AJ, the Netherlands.

[80]School of Biological, Environmental and Earth Sciences, University of Southern Mississippi; Hattiesburg, 39406, USA.

[81]Department of Forest Ecology and Management, Swedish University of Agricultural Sciences; Umeå, 901 83, Sweden.

[82]Institute of Environmental Change and Society, University of Regina; Regina, Saskatchewan, S4S0A2, Canada.

[83]Department of Ecology and Zoology, Federal University of Santa Catarina; Florianópolis, 88040-900, Brazil.

[84]Department of Biology, Memorial University of Newfoundland; St. John's, A1C5S7, Canada.

[85]Fish Science, Washington Department of Fish and Wildlife; Mill Creek, 98012, USA.

[86]US Forest Service; Hilo, 96720, USA.

[87]Department of Biological Sciences, Michigan Technological University; Houghton, 49931, USA.

[88]Department of Fisheries and Aquatic Science, University of Eldoret; Eldoret, 30100, Kenya.

[89]Department of Natural Resources and the Environment, Cornell University; Ithaca, 14853, USA.

[90]Department of Aquatic Sciences and Assessment, Swedish University of Agricultural Sciences, Uppsala, 75007, Sweden.

[91]Enviromental Microbiology Laboratory, Biology Institute; Bahia, 40170115, Brazil.

[92]Freshwater and Marine Solutions Unit, Finnish Environment Institute, Syke; Jyväskylä, 40500, Finland.

[93]Department of Biology, University of Zagreb; Zagreb, 10000, Croatia.

[94]Asian School of the Environment, Nanyang Technological University; Singapore, 639798, Singapore.

[95]Graduate School of Science and Engineering, Ehime University; Matsuyama, 790-8577, Japan.

[96]Center for Freshwater Research and Education, Lake Superior State University; Sault Sainte Marie, 49783, USA.

[97]Center for Limnology, University of Wisconsin - Madison; Madison, 53706, USA.

[98]Department of Ecology, University of the State of Rio de Janeiro; Rio de Janeiro, 20550-013, Brazil.

[99]Department of Ecology and Genetics, University of Oulu; Oulu, 90014, Finland.

[100]Faculty of Environmental Earth Science, Hokkaido University; Sapporo, 060-0810, Japan.

[101]Departamento de Ecologia, IBRAG, Universidade do Estado do Rio de Janeiro; Rio de Janeiro, 20550-900, Brazil.

[102]Department of Biological and Environmental Science, University of Jyväskylä; Jyväskylä, FI-40014, Finland.

[103]Instituto de Ciencias Marinas y Limnologicas, Universidad Austral de Chile; Valdivia, 5090000, Chile.

[104]Departent of Geography, Masaryk University Brno; Czechia, 60300, Czech Republic.

[105]Oulanka research station, University of Oulu; Kuusamo, 93900, Finland.

[106]Water, Energy and Environmental Engineering, University of Oulu; Oulu, 90014, Finland.

[107]Aquatic Ecology and Water Quality Management Group, Wageningen University; Wageningen, 6708 PB, the Netherlands.

[108]Trout Unlimited Alaska; Anchorage, 9951, USA.

[109]Centro de Investigación en Ecosistemas de la Patagonia (Centro CIEP); Coyhaique, 5950000, Chile.

[110]Department of Forest and Conservation Sciences, The University of British Columbia; Vancouver, V6T1Z4, Canada.

[111]Department of Ecology, The University of Adelaide; Adelaide, 5000, Australia.

[112]Department of Biology, Universidad del Zulia; Maracaibo, 4002, Venezuela.

[113]Department of Systems Ecology and Sustainability, University of Bucharest; Bucharest, 050095, Romania.

[114]Department of Aquatic Ecology, EAWAG; Duebendorf, 8600, Switzerland.

[115]Institute of Integrative Biology, ETH Zurich; Zurich, 8293, Switzerland.

[116]School of Public and Environmental Affairs, Indiana University; Bloomington, 47405, USA.

[117]Department of Biology, Queen's University; Kingston, K7L 3N6, Canada.

[118]PE Limnoecology Research Group, HUN-REN; Veszprém, 8200, Hungary.

[119]Research Group of Limnology, Center for Natural Science, University of Pannonia; Veszprém, 8200, Hungary.

[120]Institute of Biology, University of Latvia; Riga, LV-1004, Latvia.

[121]Department of Ecology and Environmental Science, Umeå University; Umeå, 90736, Sweden.

[122]Department of Biosciences, Mangalore University; Mangalore, 574199, India.

[123]Department of Biology, Rensselaer Polytechnic Institute; Troy, 12180, USA.

[124]Department of Geography and Environmental Systems, University of Maryland, Baltimore County; Baltimore, 21250, USA.

[125]Departamento de Ecología y Gestión Ambiental, Centro Universitario Regional del Este, UDELAR; Maldonado, CP 20000, Uruguay.

[126]School of Biological Sciences, University of Canterbury; Christchurch, 8014, New Zealand.

[127]Te Pūnaha Matatini Centre of Research Excellence, University of Canterbury; Christchurch, 8014, New Zealand.

[128]Nature Solutions, Finnish Environment Centre; Helsinki, 00790, Finland.

[129]Integrative Biology, University of Texas at San Antonio; San Antonio, 78249, USA.

[130]Chair of Hydrobiology and Fisheries, Estonian University of Life Sciences; Tartu, 51006, Estonia.

[131]EA-International; Horby, 24293, Sweden.

[132]Silviculture, Taiwan Forest Research Institute; Taipei, 100, Taiwan.

[133]Department of Biological Sciences, Virginia Tech University; Blacksburg, Virginia, 24060, USA.

[134]Department of Biology, East Stroudsburg University; East Stroudsburg, 18301, USA.

[135]Department of Biology, University of Waterloo; Waterloo, N2L 3G1, Canada.

[136]Department of Civil and Environmental Engineering, Tokyo Institute of Technology; Tokyo, 152-8550, Japan.

[137]School of Science Technology and Engineering, University of the Sunshine Coast; Sippy Downs, 4556, Australia.

[138]Research Center of Cultural Landscape Protection and Ecological Restoration, School of Architecture, Soochow University; Suzhou, 215006, China.

[139]Water Mission Area, U.S. Geological Survey; San Francisco, 94116, USA.

Materials and Methods

Cellulose decomposition

We used a global dataset of cellulose-decomposition rates generated by a coordinated field experiment (Cellulose Decomposition Experiment [CELLDEX]) (*19*). Cotton strips were incubated in 514 flowing waters spanning 135 degrees of latitude by a consortium of over 150 peer-sourced researchers. Cotton strips are composed of cellulose, the primary constituent of most terrestrially derived leaf litter and the most abundant organic polymer on Earth; as such, cellulose is a plant polymer that is highly relevant for global biogeochemical cycles. The cotton-strip assay is an integrative measure of the activity of heterotrophic microbes and is highly sensitive to an array of environmental factors including nutrient concentrations, temperature, and pollutants (*24*). As used in our study the assay is not believed to be directly influenced by the feeding activity of macroinvertebrates. Cotton strips were deployed in 2015-2016 during periods of peak organic-matter inputs to flowing waters (e.g., autumn in temperate zones, dry season in tropical deciduous forests) at sites relatively free of major anthropogenic impacts. We typically chose stream orders 1-3 (*45*) and had sites located in each of Earth's major terrestrial biomes (*19*), and the cellulose-decomposition rate at each river was summarized as the exponential decay rate (K_d) of tensile-strength loss:

$$K_d = -\ln(T_f/T_i)/t$$

where T_f is the final tensile strength of each cotton strip after incubation in the field, T_i is an average tensile-strength value of control strips not incubated in the field to establish initial tensile strength, and t the field incubation time in days (usually 21-30 days). The loss of tensile strength corresponds to the decomposition of the cotton fabric and is driven predominantly by the activity of microbes. Field and laboratory methods are detailed in (*19*, *24*).

Environmental data sources

For data on environmental variables other than *in-situ* water temperature, we relied on publicly available datasets with global coverage: 1) (*46*) for estimates of river yields of dissolved reactive phosphorus (kg DRP-P ha^{-1} yr^{-1}) and nitrate+nitrite (kg NOx-N ha^{-1} yr^{-1}); 2) (*47*) for estimates of nitrogen (N) deposition; 3) (*48*) and (*49*) for estimates of phosphorus (P) deposition that we then interpolated; and 4) (*38*) for data on 96 variables summarized at the 12-digit hydrological scale or for the area upstream (HydroRIVERS: River ATLAS_v10_lev12; HydroBASINS: BasinATLAS_v10_lev12) for either river reaches or corresponding sub-watersheds, though all variables were not populated for all sub-watersheds. We excluded variables from HydroBASINS that were composite measures where we already included confounded variables (e.g., biome, human development index, and human footprint). We recorded temperature data with loggers for a subset (n=360) of the 514 rivers to determine the mean daily temperature of the river water during the cotton-strip incubation period.

Litter decomposition data

We used a global dataset of 3,216 unique estimates of litter-decomposition rates (as K_d using the equation above except that mass rather than tensile strength was used) for 125 plant genera and multiple experimental conditions (*27*) to independently validate whether our

cellulose-decomposition model could explain rates of litter decomposition. These data are an expanded version of the data published by LeRoy et al. (2020) (see data repository for complete data)(*27*). For each unique river reach sampled in the dataset, we averaged K_d estimates by each unique combination of leaf condition (i.e., leaves picked from the trees while still living or collected from the ground after senescence), plant genus, and direct feeding by detritivorous invertebrates (i.e., coarse-mesh which included invertebrates or fine-mesh litter bags which excluded invertebrates). We excluded any data for which we had 3 or fewer measurements of decomposition for a genus. The final dataset included 895 unique observations of 35 genera from 559 river reaches. All but 7 estimates of litter decomposition also included mean temperature during deployment, which we included as a predictor variable.

Leaf- and litter-trait data sources

We downloaded 384,252 records from 21,100 plant species and 4,557 genera of leaf traits related to nutrient, micronutrient, and structural compounds for leaves from the TRY plant-trait database (*31*). After filtering for traits describing the chemical constituency of plant leaves that we felt were most relevant for decomposition, the resulting database included average values for 7 traits representing 64 genera. Litter traits were assembled from 114 studies comprising 602 litter deployments of 172 genera in rivers (*43*). These trait values were joined by genus to the aforementioned empirical data on leaf litter. All genera for which we had litter-decomposition rates had data regarding either leaf or litter traits, and most included complete values for both. Details on filtering, aggregating, and variable selection as well as full datasets can be found in the data repository (*43*).

Data Analysis

Environmental data processing

At each river sampling location in the CELLDEX dataset, we combined temperature recorded during the experiment, extracted values from nutrient yield and deposition rasters, and attributes from HydroBASINS summarized by upstream watershed as well as the containing sub-watershed. For HydroBASINS fields that were additionally available as monthly summaries (e.g., air temperature, potential evapotranspiration, snow coverage), we used both annual summaries and those from the month of deployment at each site as predictors in the BRT model. Variables from HydroBASINS were back-transformed into original units, and predictors with log-normal distributions were $\log_{10}$ transformed. In total, we had 101 predictor variables for our cellulose-decomposition model.

Boosted-regression tree models

The choice between boosted regression tree (BRT) and other modeling techniques, such as Generalized Additive Models (GAMs) or neural networks depends on the specific characteristics of the data and the goals of the analysis. For our purposes, BRTs were an appropriate tool to answer our questions while addressing some of the complexity in our data. BRTs are recognized for their predictive accuracy, particularly in managing nonlinear relationships and interactions among predictors. The method is appropriate for handling missing data and outliers and processing large datasets. As the BRT constructs trees, it selects the most informative variables at each step, and assigns lower importance to the variables that contribute

less to predictive performance. BRT is also resilient to irrelevant variables, as the boosting process assigns diminished weights to less informative variables and reduces their impact on the final model. BRTs can also capture interactions between variables and because the boosting process is adaptive, it allows the algorithm to focus on the most important variables and their interactions. Therefore, it reduces the risk of overfitting and improves the generalization of the model when challenged with new data. The learning rate of the BRT imposes a penalty on over-fitting. Learning rates are often set to between 0.01 and 0.1, and ours was set to 0.001. Smaller learning rates put a penalty on the contribution of each tree, a technique that prevents the model from fitting the training data too closely.

In BRTs, "importance" refers to the degree of influence each predictor variable has on the predictive performance of the model and is normalized so the sum of all explanatory variable importance is 100. Variable importance in BRT is calculated based on how often a given variable is selected for: 1) splitting across all the trees, and 2) how much it contributes to the reduction in the model's loss function. Variables that are frequently chosen and contribute to improving model performance are considered more important. Higher importance values indicate features that have a greater impact on making accurate predictions. Detailed descriptions of the BRT approach are found in (*50*).

We used the gbm package in R (version 4.3.2) to build BRT models (*51, 52*) for cellulose decomposition and leaf-litter decomposition. Both BRT models were fitted with Gaussian distributions, learning rates of 0.001, and an interaction depth of 5. We initially used 20,000 trees in the cellulose model and the cross-validation determined the optional number of trees was 9,497. For the litter model, we initially ran 50,000 trees, and the optimal number was identified as 40,853. While BRT models handle variables with broad ranges, we ln-transformed K_d to facilitate the interpretation of results. The cellulose model used 101 explanatory variables (table s1) and the leaf-litter model used 17 explanatory variables (table s2). We assessed model explanatory power by calculating a pseudo-R^2 for each model and determined variable importance via permutation tests (*53*) (table 1). Explanatory variables with importance values greater than $1/n_{variable}*100$ ($n_{variable}$ = total number of explanatory variables in the model) were included in trees more than would be expected from random chance and identified for further discussion (*54*). The importance threshold was 0.99 for the cellulose model and 5.88 for the leaf-litter decomposition model. For the leaf litter model, two highly correlated explanatory variables (litter C:N and litter N content) fell just below the importance threshold but were discussed further because they each exceeded the threshold in other model runs and are well known to correlate with litter decomposition rates.

Output rasters of predicted cellulose-decomposition rates

Using the BRT models and data from the assembled spatial data layers, we predicted river K_d at the extent and at the resolution of the WorldClim rasters (global with 30 arc-second resolution; https://www.worldclim.org) using the raster package in R (*55*). In these output rasters, we did not predict K_d for sub-watersheds with ≤10 ha of sub-basin area, nor for Antarctica, which is not included in HydroATLAS. Importantly, we predicted K_d using a BRT model that included variables measured at each site in the original CELLDEX experiment (i.e., water temperatures and month of deployment), but those variables were not included in the generation of the global K_d map.

Validation of cellulose and leaf-litter BRT models

The spatial structure of the cellulose and leaf-litter datasets are quite different; therefore, we used different validation approaches for the cellulose and leaf-litter models. Because of the smaller dataset and hierarchical spatial structure of the cellulose-decomposition data (i.e., multiple streams measured by each partner), we performed a "leave-one-out" validation of the BRT by running 131 iterations of the model, each excluding one partner from the dataset. The goal was to assess the model's ability to predict the data of the omitted partner, measured through the calculation of root mean square error (RMSE). The average RMSE for the leave-one-out partner analysis was 1.08; in comparison, the BRT's cross-validation, which optimizes the number of trees directly in the code, yielded an RMSE of 0.93. The range of cellulose decomposition rates was 5.1 natural log units (K_d range 0.0012–0.20 d^{-1}). This analysis indicates that the model can predict cellulose decomposition rate with an accuracy of approximately +/- 1 natural log unit and predictions in unsampled locations have similar accuracy to the model with all data included. For the larger, leaf-litter dataset compiled from published literature (n=895 decomposition rates), we randomly selected 80% of the data and used that to train the model, and we tested the model with the remaining 20% of the data. The average RMSE for the 80/20 analysis was 0.75 (n=20 random splits). In comparison, the BRT's cross-validation, which optimizes the number of trees directly in the code, yielded an RMSE of 0.76. The range of leaf litter decomposition rates was 5.9 natural log units (K_d range 0.005–0.18), which is much greater than the RMSE, indicating that the model is sufficiently accurate to make predictions of litter decomposition.

Data. All data and code for analyses and figures are available on GitHub (*43*).

Supplemental Acknowledgements: Any use of trade, firm, or product names is for descriptive purposes only and does not imply endorsement by the U.S. Government.

Table S1.
Boosted-regression tree model importance values for cellulose decomposition rates (ln[K_d])), their description and the source of data. Importance values greater than 0.99 indicate that the variable was selected more than expected from random chance. The detailed information from the predictor variables derived from HydroBASINS can be found on their website. Variables that have similar names are typically referring to differences in the spatial or temporal characteristics of the variable. For example, air temperature tmp_dc_uyr is the annual average temperature for the total watershed upstream of sub-basin pour point, whereas tmp_dc_smx is the annual average temperature at the sub-basins pour point. If data were log transformed, "log", is written before the predictor variable text. The "Source" column denotes the origin of the data.

Boosted-regression tree - explaining cotton decomposition rate (ln[K_d])			
R^2	0.81		
Predictor variable	**Relative importance**	**Description**	**Source**
mean_mean_daily_temp	14.02	mean_mean_daily_temp	CELLDEX (*19*)
log10lka_pc_sse	6.94	Limnicity (Percent Lake Area): Category = Hydrology; Spatial Extent = {s} at sub-basin pour point; Dimensions = {se} spatial extent (%)	HydroBASINS
log10NO3c	6.7	NO3 yield	McDowell et al. 2021 (*46*)
log10DRPc	4.89	DRP yield	McDowell et al. 2021 (*46*)
AETmonth	4.4	AET month of deployment	HydroBASINS
tmp_dc_uyr	2.48	Air Temperature: Category = Climate; Spatial Extent = {u} in total watershed upstream of sub-basin pour point; Dimensions = {yr} annual average	HydroBASINS
snowmonth	2.26	Snow cover month of deployment	HydroBASINS
tmp_dc_smx	2.25	Air Temperature: Category = Climate; Spatial Extent = {s} at sub-basin pour point; Dimensions = {mx} annual maximum	HydroBASINS
soc_th_uav	2.16	Organic Carbon Content in Soil: Category = Soils & Geology; Spatial Extent = {u} in total watershed upstream of sub-basin pour point; Dimensions = {av} average	HydroBASINS

run_mm_syr	2.1	Land Surface Runoff: Category = Hydrology; Spatial Extent = {s} at sub-basin pour point; Dimensions = {yr} annual average	HydroBASINS
crp_pc_sse	2.03	Cropland Extent: Category = Landcover; Spatial Extent = {s} at sub-basin pour point; Dimensions = {se} spatial extent (%)	HydroBASINS
log10dis_m3_pmn	1.94	Natural Discharge: Category = Hydrology; Spatial Extent = {p} at sub-basin pour point; Dimensions = {mn} annual minimum	HydroBASINS
gdp_ud_sav	1.71	Gross Domestic Product: Category = Anthropogenic; Spatial Extent = {s} at sub-basin pour point; Dimensions = {av} average	HydroBASINS
slp_dg_sav	1.54	Terrain Slope: Category = Physiography; Spatial Extent = {s} at sub-basin pour point; Dimensions = {av} average	HydroBASINS
pet_mm_uyr	1.44	Potential Evapotranspiration: Category = Climate; Spatial Extent = {u} in total watershed upstream of sub-basin pour point; Dimensions = {yr} annual average	HydroBASINS
log10sgr_dk_sav	1.3	Stream Gradient: Category = Physiography; Spatial Extent = {s} at sub-basin pour point; Dimensions = {av} average	HydroBASINS
log10dor_pc_pva	1.29	Degree of Regulation: Category = Hydrology; Spatial Extent = {p} at sub-basin pour point; Dimensions = {va} value	HydroBASINS
log10pop_ct_usu	1.29	Population Count: Category = Anthropogenic; Spatial Extent = {u} in total watershed upstream of sub-basin pour point; Dimensions = {su} sum	HydroBASINS
tempmonth	1.28	Air temp month of deployment	HydroBASINS
tmp_dc_syr	1.28	Air Temperature: Category = Climate; Spatial Extent = {s} at sub-basin pour point; Dimensions = {yr} annual average	HydroBASINS
crp_pc_use	1.24	Cropland Extent: Category = Landcover; Spatial Extent = {u} in	HydroBASINS

		total watershed upstream of sub-basin pour point; Dimensions = {se} spatial extent (%)	
ele_mt_smx	1.22	Elevation: Category = Physiography; Spatial Extent = {s} at sub-basin pour point; Dimensions = {mx} maximum	HydroBASINS
log10dis_m3_pyr	1.09	Natural Discharge: Category = Hydrology; Spatial Extent = {p} at sub-basin pour point; Dimensions = {yr} annual average	HydroBASINS
snd_pc_uav	1.09	Sand Fraction in Soil: Category = Soils & Geology; Spatial Extent = {u} in total watershed upstream of sub-basin pour point; Dimensions = {av} average	HydroBASINS
log10rdd_mk_uav	1.07	Road Density: Category = Anthropogenic; Spatial Extent = {u} in total watershed upstream of sub-basin pour point; Dimensions = {av} average	HydroBASINS
tmp_dc_smn	1.01	Air Temperature: Category = Climate; Spatial Extent = {s} at sub-basin pour point; Dimensions = {mn} annual minimum	HydroBASINS
TNdep	0.95	TN deposition	Ackerman et al. 2019 (*47*)
pac_pc_sse	0.9	Protected Area Extent: Category = Landcover; Spatial Extent = {s} at sub-basin pour point; Dimensions = {se} spatial extent (%)	HydroBASINS
pre_mm_uyr	0.89	Precipitation: Category = Climate; Spatial Extent = {u} in total watershed upstream of sub-basin pour point; Dimensions = {yr} annual average	HydroBASINS
aet_mm_uyr	0.88	Actual Evapotranspiration: Category = Climate; Spatial Extent = {u} in total watershed upstream of sub-basin pour point; Dimensions = {yr} annual average	HydroBASINS
log10gdp_ud_usu	0.88	Gross Domestic Product: Category = Anthropogenic; Spatial Extent = {u} in total watershed upstream of sub-	HydroBASINS

		basin pour point; Dimensions = {su} sum	
log10lkv_mc_usu	0.85	Lake Volume: Category = Hydrology; Spatial Extent = {u} in total watershed upstream of sub-basin pour point; Dimensions = {su} sum	HydroBASINS
pre_mm_syr	0.85	Precipitation: Category = Climate; Spatial Extent = {s} at sub-basin pour point; Dimensions = {yr} annual average	HydroBASINS
TPdep	0.79	TP deposition	Brahney et al. 2015 (*48*) & Mahowald 2008 (*49*)
log10ppd_pk_uav	0.78	Population Density: Category = Anthropogenic; Spatial Extent = {u} in total watershed upstream of sub-basin pour point; Dimensions = {av} average	HydroBASINS
cly_pc_sav	0.77	Clay Fraction in Soil: Category = Soils & Geology; Spatial Extent = {s} at sub-basin pour point; Dimensions = {av} average	HydroBASINS
moist_indexmonth	0.77	moist_indexmonth	HydroBASINS
nli_ix_sav	0.7	Nighttime Lights: Category = Anthropogenic; Spatial Extent = {s} at sub-basin pour point; Dimensions = {av} average	HydroBASINS
ele_mt_sav	0.68	Elevation: Category = Physiography; Spatial Extent = {s} at sub-basin pour point; Dimensions = {av} average	HydroBASINS
ari_ix_uav	0.67	Global Aridity Index: Category = Climate; Spatial Extent = {u} in total watershed upstream of sub-basin pour point; Dimensions = {av} average	HydroBASINS
soc_th_sav	0.66	Organic Carbon Content in Soil: Category = Soils & Geology; Spatial Extent = {s} at sub-basin pour point; Dimensions = {av} average	HydroBASINS
snw_pc_uyr	0.65	Snow Cover Extent: Category = Climate; Spatial Extent = {u} in total watershed upstream of sub-basin	HydroBASINS

		pour point; Dimensions = {yr} annual average	
log10rev_mc_usu	0.63	Reservoir Volume: Category = Hydrology; Spatial Extent = {u} in total watershed upstream of sub-basin pour point; Dimensions = {su} sum	HydroBASINS
log10gdp_ud_ssu	0.62	Gross Domestic Product: Category = Anthropogenic; Spatial Extent = {s} at sub-basin pour point; Dimensions = {su} sum	HydroBASINS
PETmonth	0.61	PET month of deployment	HydroBASINS
log10rdd_mk_sav	0.59	Road Density: Category = Anthropogenic; Spatial Extent = {s} at sub-basin pour point; Dimensions = {av} average	HydroBASINS
slt_pc_sav	0.59	Silt Fraction in Soil: Category = Soils & Geology; Spatial Extent = {s} at sub-basin pour point; Dimensions = {av} average	HydroBASINS
pac_pc_use	0.58	Protected Area Extent: Category = Landcover; Spatial Extent = {u} in total watershed upstream of sub-basin pour point; Dimensions = {se} spatial extent (%)	HydroBASINS
slp_dg_uav	0.57	Terrain Slope: Category = Physiography; Spatial Extent = {u} in total watershed upstream of sub-basin pour point; Dimensions = {av} average	HydroBASINS
for_pc_use	0.56	Forest Cover Extent: Category = Landcover; Spatial Extent = {u} in total watershed upstream of sub-basin pour point; Dimensions = {se} spatial extent (%)	HydroBASINS
gwt_cm_sav	0.55	Groundwater Table Depth: Category = Hydrology; Spatial Extent = {s} at sub-basin pour point; Dimensions = {av} average	HydroBASINS
log10inu_pc_ult	0.55	Inundation Extent: Category = Hydrology; Spatial Extent = {u} in total watershed upstream of sub-basin pour point; Dimensions = {lt} long-term maximum	HydroBASINS

ele_mt_uav	0.52	Elevation: Category = Physiography; Spatial Extent = {u} in total watershed upstream of sub-basin pour point; Dimensions = {av} average	HydroBASINS
cly_pc_uav	0.51	Clay Fraction in Soil: Category = Soils & Geology; Spatial Extent = {u} in total watershed upstream of sub-basin pour point; Dimensions = {av} average	HydroBASINS
for_pc_sse	0.5	Forest Cover Extent: Category = Landcover; Spatial Extent = {s} at sub-basin pour point; Dimensions = {se} spatial extent (%)	HydroBASINS
log10ria_ha_ssu	0.5	River Area: Category = Hydrology; Spatial Extent = {s} at sub-basin pour point; Dimensions = {su} sum	HydroBASINS
precipmonth	0.48	Precipitation month of deployment	HydroBASINS
pst_pc_use	0.47	Pasture Extent: Category = Landcover; Spatial Extent = {u} in total watershed upstream of sub-basin pour point; Dimensions = {se} spatial extent (%)	HydroBASINS
snd_pc_sav	0.47	Sand Fraction in Soil: Category = Soils & Geology; Spatial Extent = {s} at sub-basin pour point; Dimensions = {av} average	HydroBASINS
log10pop_ct_ssu	0.45	Population Count: Category = Anthropogenic; Spatial Extent = {s} at sub-basin pour point; Dimensions = {su} sum	HydroBASINS
aet_mm_syr	0.43	Actual Evapotranspiration: Category = Climate; Spatial Extent = {s} at sub-basin pour point; Dimensions = {yr} annual average	HydroBASINS
snw_pc_smx	0.43	Snow Cover Extent: Category = Climate; Spatial Extent = {s} at sub-basin pour point; Dimensions = {mx} annual maximum	HydroBASINS
log10ero_kh_sav	0.38	Soil Erosion: Category = Soils & Geology; Spatial Extent = {s} at sub-basin pour point; Dimensions = {av} average	HydroBASINS
ari_ix_sav	0.36	Global Aridity Index: Category = Climate; Spatial Extent = {s} at sub-	HydroBASINS

		basin pour point; Dimensions = {av} average	
log10ero_kh_uav	0.35	Soil Erosion: Category = Soils & Geology; Spatial Extent = {u} in total watershed upstream of sub-basin pour point; Dimensions = {av} average	HydroBASINS
swc_pc_syr	0.35	Soil Water Content: Category = Soils & Geology; Spatial Extent = {s} at sub-basin pour point; Dimensions = {yr} annual average	HydroBASINS
log10dis_m3_pmx	0.33	Natural Discharge: Category = Hydrology; Spatial Extent = {p} at sub-basin pour point; Dimensions = {mx} annual maximum	HydroBASINS
cmi_ix_uyr	0.32	Climate Moisture Index: Category = Climate; Spatial Extent = {u} in total watershed upstream of sub-basin pour point; Dimensions = {yr} annual average	HydroBASINS
slt_pc_uav	0.32	Silt Fraction in Soil: Category = Soils & Geology; Spatial Extent = {u} in total watershed upstream of sub-basin pour point; Dimensions = {av} average	HydroBASINS
log10ppd_pk_sav	0.31	Population Density: Category = Anthropogenic; Spatial Extent = {s} at sub-basin pour point; Dimensions = {av} average	HydroBASINS
ele_mt_smn	0.3	Elevation: Category = Physiography; Spatial Extent = {s} at sub-basin pour point; Dimensions = {mn} minimum	HydroBASINS
pet_mm_syr	0.29	Potential Evapotranspiration: Category = Climate; Spatial Extent = {s} at sub-basin pour point; Dimensions = {yr} annual average	HydroBASINS
log10lka_pc_use	0.26	Limnicity (Percent Lake Area): Category = Hydrology; Spatial Extent = {u} in total watershed upstream of sub-basin pour point; Dimensions = {se} spatial extent (%)	HydroBASINS
log10riv_tc_usu	0.26	River Volume: Category = Hydrology; Spatial Extent = {u} in total watershed upstream of sub-	HydroBASINS

		basin pour point; Dimensions = {su} sum	
soilwatermonth	0.26	Soil water % month of deployment	HydroBASINS
log10ria_ha_usu	0.21	River Area: Category = Hydrology; Spatial Extent = {u} in total watershed upstream of sub-basin pour point; Dimensions = {su} sum	HydroBASINS
log10riv_tc_ssu	0.2	River Volume: Category = Hydrology; Spatial Extent = {s} at sub-basin pour point; Dimensions = {su} sum	HydroBASINS
nli_ix_uav	0.18	Nighttime Lights: Category = Anthropogenic; Spatial Extent = {u} in total watershed upstream of sub-basin pour point; Dimensions = {av} average	HydroBASINS
kar_pc_sse	0.17	Karst Area Extent: Category = Soils & Geology; Spatial Extent = {s} at sub-basin pour point; Dimensions = {se} spatial extent (%)	HydroBASINS
pst_pc_sse	0.17	Pasture Extent: Category = Landcover; Spatial Extent = {s} at sub-basin pour point; Dimensions = {se} spatial extent (%)	HydroBASINS
log10inu_pc_umx	0.16	Inundation Extent: Category = Hydrology; Spatial Extent = {u} in total watershed upstream of sub-basin pour point; Dimensions = {mx} annual maximum	HydroBASINS
urb_pc_sse	0.16	Urban Extent: Category = Anthropogenic; Spatial Extent = {s} in reach catchment; Dimensions = {se} spatial extent (%)	HydroBASINS
log10inu_pc_smx	0.14	Inundation Extent: Category = Hydrology; Spatial Extent = {s} at sub-basin pour point; Dimensions = {mx} annual maximum	HydroBASINS
snw_pc_syr	0.14	Snow Cover Extent: Category = Climate; Spatial Extent = {s} at sub-basin pour point; Dimensions = {yr} annual average	HydroBASINS
ire_pc_sse	0.12	Irrigated Area Extent (Equipped): Category = Landcover; Spatial Extent = {s} at sub-basin pour point; Dimensions = {se} spatial extent (%)	HydroBASINS

kar_pc_use	0.12	Karst Area Extent: Category = Soils & Geology; Spatial Extent = {u} in total watershed upstream of sub-basin pour point; Dimensions = {se} spatial extent (%)	HydroBASINS
swc_pc_uyr	0.12	Soil Water Content: Category = Soils & Geology; Spatial Extent = {u} in total watershed upstream of sub-basin pour point; Dimensions = {yr} annual average	HydroBASINS
cmi_ix_syr	0.1	Climate Moisture Index: Category = Climate; Spatial Extent = {s} at sub-basin pour point; Dimensions = {yr} annual average	HydroBASINS
ire_pc_use	0.1	Irrigated Area Extent (Equipped): Category = Landcover; Spatial Extent = {u} in total watershed upstream of sub-basin pour point; Dimensions = {se} spatial extent (%)	HydroBASINS
log10inu_pc_slt	0.1	Inundation Extent: Category = Hydrology; Spatial Extent = {s} at sub-basin pour point; Dimensions = {lt} long-term maximum	HydroBASINS
wet_pc_ug1	0.1	Wetland Extent: Category = Landcover; Spatial Extent = {u} in total watershed upstream of sub-basin pour point; Dimensions = {g1} Wetland class grouping; see https://www.worldwildlife.org/pages/global-lakes-and-wetlands-database	HydroBASINS
urb_pc_use	0.08	Urban Extent: Category = Anthropogenic; Spatial Extent = {u} in total watershed upstream of sub-basin pour point; Dimensions = {se} spatial extent (%)	HydroBASINS
log10inu_pc_umn	0.07	Inundation Extent: Category = Hydrology; Spatial Extent = {u} in total watershed upstream of sub-basin pour point; Dimensions = {mn} annual minimum	HydroBASINS
wet_pc_ug2	0.07	Wetland Extent: Category = Landcover; Spatial Extent = {u} in total watershed upstream of sub-basin pour point; Dimensions = {g2} Wetland class grouping; see	HydroBASINS

		https://www.worldwildlife.org/pages/global-lakes-and-wetlands-database	
log10inu_pc_smn	0.06	Inundation Extent: Category = Hydrology; Spatial Extent = {s} at sub-basin pour point; Dimensions = {mn} annual minimum	HydroBASINS
wet_pc_sg1	0.05	Wetland Extent: Category = Landcover; Spatial Extent = {s} at sub-basin pour point; Dimensions = {g1} Wetland class grouping; see https://www.worldwildlife.org/pages/global-lakes-and-wetlands-database	HydroBASINS
prm_pc_use	0.02	Permafrost Extent: Category = Landcover; Spatial Extent = {u} in total watershed upstream of sub-basin pour point; Dimensions = {se} spatial extent (%)	HydroBASINS
wet_pc_sg2	0.01	Wetland Extent: Category = Landcover; Spatial Extent = {s} at sub-basin pour point; Dimensions = {g2} Wetland class grouping; see https://www.worldwildlife.org/pages/global-lakes-and-wetlands-database	HydroBASINS
gla_pc_sse	0	Glacier Extent: Category = Landcover; Spatial Extent = {s} at sub-basin pour point; Dimensions = {se} spatial extent (%)	HydroBASINS
gla_pc_use	0	Glacier Extent: Category = Landcover; Spatial Extent = {u} in total watershed upstream of sub-basin pour point; Dimensions = {se} spatial extent (%)	HydroBASINS
prm_pc_sse	0	Permafrost Extent: Category = Landcover; Spatial Extent = {s} at sub-basin pour point; Dimensions = {se} spatial extent (%)	HydroBASINS

Table S2.

Boosted-regression tree model importance values for leaf-litter decomposition rates (ln[*Kd*]), their description and the source of data. Importance values greater than 5.88 indicate that the variable was selected more than expected from random chance. Additional information about plant traits can be found in the data repository (*43*) in the file "Litter_trait_review.csv" and more details about the TRY database are contained in (*31*).

Boosted-regression tree - explaining leaf litter decomposition rate (ln[K_d])			
R^2	0.70		
Predictor variable	Relative importance	Description	Source
ln_pred_kd	39.47	Model predicted cotton kd	This study
Mesh.size	20.84	Mesh size	LeRoy et al. 2020 (*27*)
Lignin_Litter_Mn	11.96	Litter lignin content	Literature values (*43*)
CtoN_Litter_Mn	5.45	Litter C:N	Literature values (*43*)
N_Litter_Mn	5.23	Litter N content	Literature values (*43*)
P_Litter_Mn	3.59	Litter P content	Literature values (*43*)
C_Litter_Mn	2.37	Litter C content	Literature values (*43*)
Cellulose_Litter_Mn	2.20	Litter cellulose content	Literature values (*43*)
Ca_Leaf_Mn	2.03	Leaf Ca content	TRY database
NtoP_Leaf_Mn	1.19	Leaf N:P	TRY database
Thick_Mn	1.04	Leaf thickness	TRY database
Leaf.condition	1.03	Leaf condition	TRY database
NtoP_Litter_Mn	0.95	Litter N:P	Literature values (*43*)
P_Leaf_Mn	0.76	Leaf P content	TRY database
CtoN_Leaf_Mn	0.69	Leaf C:N	TRY database
C_Leaf_Mn	0.66	Leaf C content	TRY database
N_Leaf_Mn	0.53	Leaf N content	TRY database

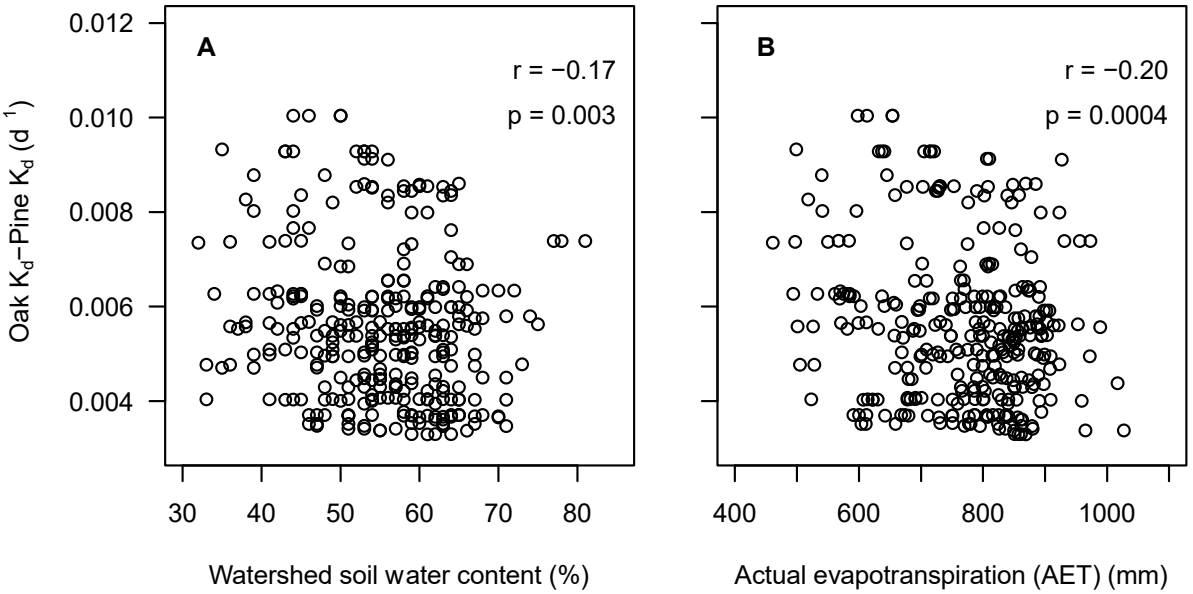

Fig. S1.

Correlation plots of the relationship between the magnitude of predicted change in litter-decomposition rates in pine-dominated forests invaded by the pine bark beetle and watershed soil water content (A) and AET (B). Greater values indicate a higher magnitude increase in litter decomposition upon canopy replacement. Our forecasts predict insect-induced canopy replacement from pine to oak would approximately double mean decomposition rates (see main text). Though the relationships are highly variable, the associations between the predicted magnitude of change in decomposition and soil water and AET indicate drier subwatersheds are expected to have a larger change in decay rates than wetter sites.

References in Supplemental Files Only: References *45–55* are referenced only in the Supplemental Materials.